

International Ocean Discovery Program Expedition 399 Scientific Prospectus

Building Blocks of Life, Atlantis Massif

Andrew McCaig
Co-Chief Scientist
School of Earth and Environment
University of Leeds
United Kingdom

Susan Q. Lang
Co-Chief Scientist
Department of Geology and Geophysics
Woods Hole Oceanographic Institution
USA

Peter Blum
Expedition Project Manager/Staff Scientist
International Ocean Discovery Program
Texas A&M University
USA

Publisher's notes

This publication was prepared by the *JOIDES Resolution* Science Operator (JRSO) at Texas A&M University (TAMU) as an account of work performed under the International Ocean Discovery Program (IODP). This material is based upon work supported by the JRSO, which is a major facility funded by the National Science Foundation Cooperative Agreement Number OCE1326927. Funding for IODP is provided by the following international partners:

National Science Foundation (NSF), United States
Ministry of Education, Culture, Sports, Science and Technology (MEXT), Japan
European Consortium for Ocean Research Drilling (ECORD)
Ministry of Science and Technology (MOST), People's Republic of China
Australia-New Zealand IODP Consortium (ANZIC)
Ministry of Earth Sciences (MoES), India

Portions of this work may have been published in whole or in part in other IODP documents or publications.

This IODP *Scientific Prospectus* is based on pre-cruise *JOIDES Resolution* Facility advisory panel discussions and scientific input from the designated Co-Chief Scientists on behalf of the drilling proponents. During the course of the cruise, actual site operations may indicate to the Co-Chief Scientists, the Expedition Project Manager/Staff Scientist, and the Operations Superintendent that it would be scientifically or operationally advantageous to amend the plan detailed in this prospectus. It should be understood that any substantial changes to the science deliverables outlined in the plan presented here are contingent upon the approval of the IODP JRSO Director and/or *JOIDES Resolution* Facility Board.

Disclaimer

The JRSO is supported by the NSF. Any opinions, findings, and conclusions or recommendations expressed in this material do not necessarily reflect the views of the NSF, the participating agencies, TAMU, or Texas A&M Research Foundation.

Copyright

Except where otherwise noted, this work is licensed under the Creative Commons Attribution 4.0 International (CC BY 4.0) license (<https://creativecommons.org/licenses/by/4.0/>). Unrestricted use, distribution, and reproduction are permitted, provided the original author and source are credited.



Citation

McCaig, A., Lang, S.Q., and Blum, P., 2022. Expedition 399 Scientific Prospectus: Building Blocks of Life, Atlantis Massif. International Ocean Discovery Program. <https://doi.org/10.14379/iodp.sp.399.2022>

ISSN

World Wide Web: 2332-1385

Abstract

International Ocean Discovery Program (IODP) Expedition 399 will collect new cores from the Atlantis Massif (30°N; Mid-Atlantic Ridge), an oceanic core complex that has transformed our understanding of tectonic and magmatic processes at slow- and ultraslow-spreading ridges. The exposure of deep mantle rocks leads to serpentinization, with major consequences for the properties of the oceanic lithosphere, heat exchange between the ocean and crust, geochemical cycles, and microbial activity. The Lost City hydrothermal field (LCHF) is situated on its southern wall and vents warm (40°–95°C) alkaline fluids rich in hydrogen, methane, and abiotic organic molecules. The Atlantis Massif was the site of four previous expeditions (Integrated Ocean Drilling Program Expeditions 304, 305, and 340T and IODP Expedition 357) and numerous dredging and submersible expeditions. The deepest IODP hole in young (<2 My) oceanic lithosphere, Hole U1309D, was drilled 5 km north of the LCHF and reaches 1415 meters below seafloor (mbsf) through a primitive series of gabbroic rock. In contrast, during Expedition 357 a series of shallow (<16.4 mbsf) holes were drilled along the south wall of the massif, one within 0.4 km of the LCHF, and serpentinized peridotites were recovered. The hydrologic regime differs between the two locations, with a low permeability conductive regime in Hole U1309D and a high likelihood of deep permeability along the southern wall.

Expedition 399 targets both locations to collect new data on ancient processes during deformation and alteration of detachment fault rocks. Recovered rocks and fluids will provide new insights into ongoing water-rock interactions, abiotic organic synthesis reactions, and the extent and diversity of life in the subseafloor in an actively serpentinizing system. We will deepen Hole U1309D to 2060 mbsf, where temperatures are expected to be ~220°C. The lithology is predicted to transition with depth from primarily gabbroic to more ultramafic material. Predicted temperatures are well above the known limits of life, so detectable hydrogen, methane, and organic molecules can be readily attributed to abiotic processes. A new ~200 m hole will be drilled on the southern ridge close to Expedition 357 Site M0069, where both deformed and undeformed serpentinites were recovered. We aim to recover a complete section through the detachment fault zone and to sample material that reflects the subseafloor biological, geochemical, and alteration processes that occur along the LCHF circulation pathway. Borehole fluids from both holes will be collected using both the Kuster Flow Through Sampler tool and the new Multi-Temperature Fluid Sampler tool. Wire-line logging will provide information on downhole density and resistivity, image structural features, and document fracture orientations. A reentry system will be installed at proposed Site AMDH-02A, and Hole U1309D will be left open for future deep drilling, fluid sampling, and potentially borehole observatories.

Plain language summary

Where most of us live, on the continents, the Earth's crust is normally 30–40 kilometers thick, and the underlying mantle cannot be reached by drilling. The crust is thinner underneath the oceans, typically 6–7 kilometers thick, but still no hole has yet been drilled through normal thickness crust and into the mantle. Seafloor spreading at mid-ocean ridges is normally a magmatic process: the crust is continually formed by eruption and intrusion, leaving a well-layered structure with volcanics underlain by sheeted dikes and then gabbros. However, in some places magmatism cannot keep up with the spreading rate, and large convex-up extensional faults expose mantle rocks and lower crustal gabbros on the seafloor. An underwater dome-shaped mountain formed by this process is called an oceanic core complex, and these locations allow us to directly sample mantle rocks and gabbros by drilling.

The Atlantis Massif is an oceanic core complex at 30°N on the Mid-Atlantic Ridge on the north side of the Atlantis I transform fault, which offsets the ridge by ~60 kilometers. The massif is capped by a corrugated fault zone, and is composed of a large gabbro intrusion into serpentinized mantle rocks to the south. These altered mantle rocks host the Lost City hydrothermal field, which is famous for carbonate chimneys the height of a house, venting alkaline fluids rich in hydrogen and methane. The hydrogen is formed by the reaction between seawater and mantle mineral olivine, and is a powerful source of energy that may have fueled the formation of the first building blocks of life on Earth. Before life could begin, small organic molecules must have formed abiotically. Scientists have suggested that vent fields such as Lost City may be an analog of systems where these prebiotic reactions occurred, leading to the early development of life. Similar systems may be present on “icy worlds” such as Enceladus, which is one of the moons of Saturn, and capable of supporting life.

One of the main aims of International Ocean Discovery Program Expedition 399 is to study the reactions between olivine and seawater that are believed to be actively occurring at depth in the massif today. We will deepen an existing hole (U1309D) that reaches 1415 meters below the seafloor and has a bottom temperature of 140°C. This temperature is above the currently known limit for microbial life, so we can be sure that any hydrogen, methane, or organic molecules produced at greater depths are not due to microbial processes. We hope to reach 2060 meters below the seafloor, where temperatures of ~220°C are predicted. We will sample fluids in the borehole to look at active exchange of chemical components between fluid and rock and production of hydrogen and methane. We will also drill a shallow hole closer to the hydrothermal field that we predict will access the subseafloor environments that reflect the processes leading to this remarkable system.

Other aims of the expedition are to study the processes of formation of the Atlantis Massif, including magmatism, deformation, and high temperature seawater-rock interaction, as well as the microbes living within the rocks and in the borehole waters. These are “extremophile” microbes that can live in highly alkaline environments at temperatures up to 100°C and high pressures. If environments similar to Lost City were the cradle of life, this is the type of life that would have formed.

1. Schedule for Expedition 399

International Ocean Discovery Program (IODP) Expedition 399 is based on IODP drilling Proposals 937-Full2 and 937-Add (available at http://iodp.tamu.edu/scienceops/expeditions/atlantis_massif_blocks_of_life.html). Following evaluation by the IODP Scientific Advisory Structure, the expedition was scheduled for the research vessel (R/V) *JOIDES Resolution*, operating under contract with the *JOIDES Resolution* Science Operator (JRSO). At the time of publication of this *Scientific Prospectus*, the expedition is scheduled to start in Ponta Delgada (Azores, Portugal) on 12 April 2023 and to end in Ponta Delgada on 12 June (Figure F1; Table T1). The plan currently calls for 61 days of operations: ~5 days in port, ~7 days in transit, and ~49 days on site (for the current detailed schedule, see <http://iodp.tamu.edu/scienceops>). Further details about the facilities aboard *JOIDES Resolution* can be found at <http://iodp.tamu.edu/labs/index.html>.

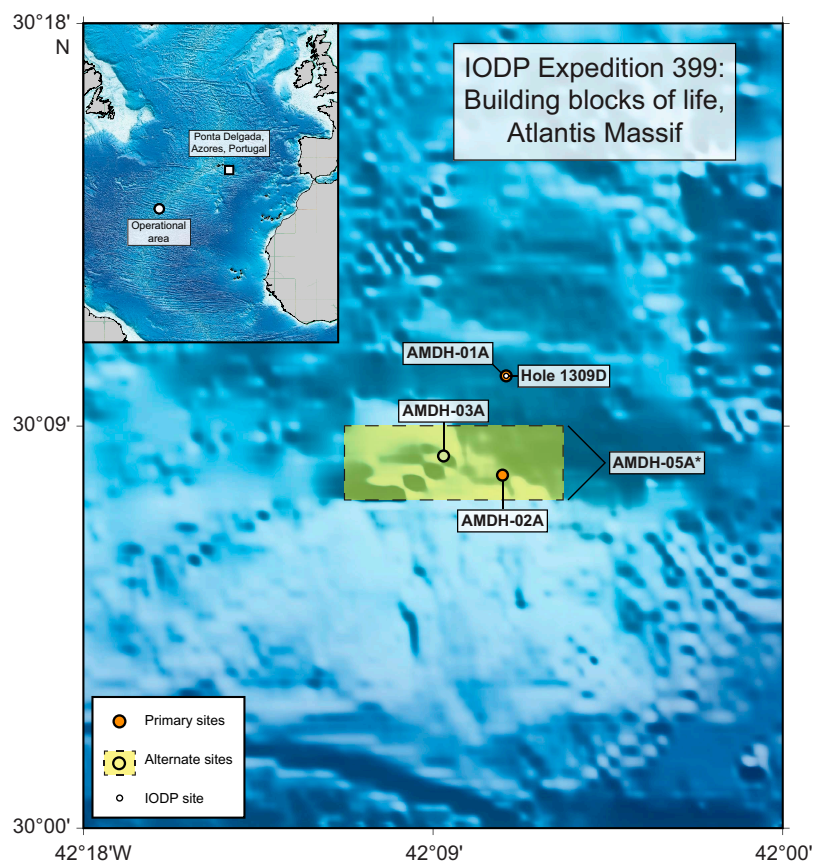


Figure F1. Location of Expedition 399 proposed primary Sites AMDH-01A and AMDH-02A, proposed alternate Sites AMDH-03A and AMDH-05A, and Hole U1309D. Inset shows operational area and Ponta Delgada, Azores (Portugal) (expedition start and end port). Shaded rectangle = Site AMDH-05A area for which the Environmental Protection and Safety Panel (EPSP) has approved operations. If this contingency is implemented, a camera survey would determine the exact location(s) where single-bit hole(s) would be drilled.

Table T1. Operations plan, Expedition 399. * = discretion of the shipboard party to deepen the hole if time is available. mbrf = meters below rig floor. EPSP = Environmental Protection and Safety Panel.

Site	Location (latitude, longitude)	Seafloor depth (mbrf)	Operations description	Transit (days)	Drilling/coring (days)	Logging (days)
Ponta Delgada			Begin expedition	5.0	Port call days	
Transit ~936 nmi to AMDH-02A @ 10.5 kt				3.7		
<u>AMDH-02A</u>	30.131700°N	836	Hole A - Seafloor survey for Hole A and pilot hole	0	1.5	0.0
EPSP	42.120200°W		Hole B - Reentry system for Hole B	0	1.6	0.0
to 800 mbsf*			Hole B - Coring bit Run 1 - to 100 mbsf	0	2.1	0.0
			Hole B - Coring bit Run 2 - to 200 mbsf	0	2.1	0.0
<u>Subtotal days on site:</u>				7.3		
Transit ~2 nmi to U1309D @ 10.5 kt				0.0		
<u>U1309</u>	30.168658°N	1656	Hole D - Fluid sampling and temperature logging	0	0.0	1.0
EPSP	42.118552°W		Hole D - Fish caliper with RCJB in U1309D to 1415.5 mbsf	0	0.8	0.0
to 2100 mbsf*			Hole D - Bit Run 1 - to 1495.5 mbsf - 2 m/h penetration rate	0	3.3	0.0
			Hole D - Bit Run 2 - to 1575.5 mbsf - 2 m/h penetration rate	0	3.3	0.0
			Hole D - Bit Run 3 - to 1655.5 mbsf - 2 m/h penetration rate	0	3.4	0.0
			Hole D - Bit Run 4 - to 1735.5 mbsf - 2 m/h penetration rate	0	3.4	0.0
			Hole D - Bit Run 5 - to 1800.0 mbsf - 1.5 m/h penetration rate	0	3.3	0.0
			Hole D - Bit Run 6 - to 1860.0 mbsf - 1.5 m/h penetration rate	0	3.2	0.0
			Hole D - Bit Run 7 - to 1920.0 mbsf - 1.5 m/h penetration rate	0	3.3	0.0
			Hole D - Bit Run 8 - to 1980.0 mbsf - 1.5 m/h penetration rate	0	3.3	0.0
			Hole D - Bit Run 9 - to 2020.0 mbsf - 1.0 m/h penetration rate	0	3.0	0.0
			Hole D - Bit Run 10 - to 2060.0 mbsf, log with triple combo, FMS-sonic, and VSI	0	3.4	1.5
			Hole E - RCB coring to 80 mbsf	0	1.8	0.0
<u>Subtotal days on site:</u>				38.1		
Transit ~2 nmi to AMDH-02A @ 10.5 kt				0.0		
<u>AMDH-02A</u>	30.131700°N	836	Hole B - Logging and fluid sampling at AMDH-02A	0	0.5	0.8
EPSP	42.120200°W					
to 800 mbsf*						
<u>Subtotal days on site:</u>				1.2		
Transit ~936 nmi to Ponta Delgada @ 10.5 kt				3.7		
Ponta Delgada			End expedition	7.5	43.3	3.3

Port call days:	5.0	Total operating days:	54.1
Subtotal days on site:	46.6	Total expedition days:	59.1

2. Introduction

The Atlantis Massif oceanic core complex (OCC) (30°N; Mid-Atlantic Ridge; Figure F2) has been investigated during four expeditions (Integrated Ocean Drilling Program Expeditions 304, 305, and 340T and IODP Expedition 357) and numerous other cruises (Cann, 1997; Blackman et al., 1998; Kelley et al., 2001, 2005; Blackman et al., 2002, 2013; Karson et al., 2006; Canales et al., 2004, 2008). The southern wall of the massif hosts the Lost City hydrothermal field (LCHF), which has vented alkaline fluids rich in H₂ and CH₄ at temperatures of 40°–90°C for >100,000 y (Ludwig et al., 2011; Kelley et al., 2005; Proskurowski et al., 2008). The LCHF is a model site for studying the serpentinization processes that lead to the creation of alkaline hydrothermal fluids rich in H₂ and CH₄, which are proposed to occur on other planetary bodies and potentially could support life. The Atlantis Massif is also a target location for return expeditions because of the ability to examine detachment fault processes that lead to ocean core complex formation. Although previous expeditions to this site have sought to characterize these serpentinization and fault deformation processes, drilling has yet to recover deep highly serpentinized material that is characteristic of the conditions thought to occur beneath the LCHF. To address these gaps in knowledge, IODP Proposal 937 argued to return to the massif to collect deeper cores both from Integrated Ocean Drilling Program Hole U1309D as well as from the southern wall in the footprint of shallower drilling done during Expedition 357 (Figures F2, F3, F4, F5).

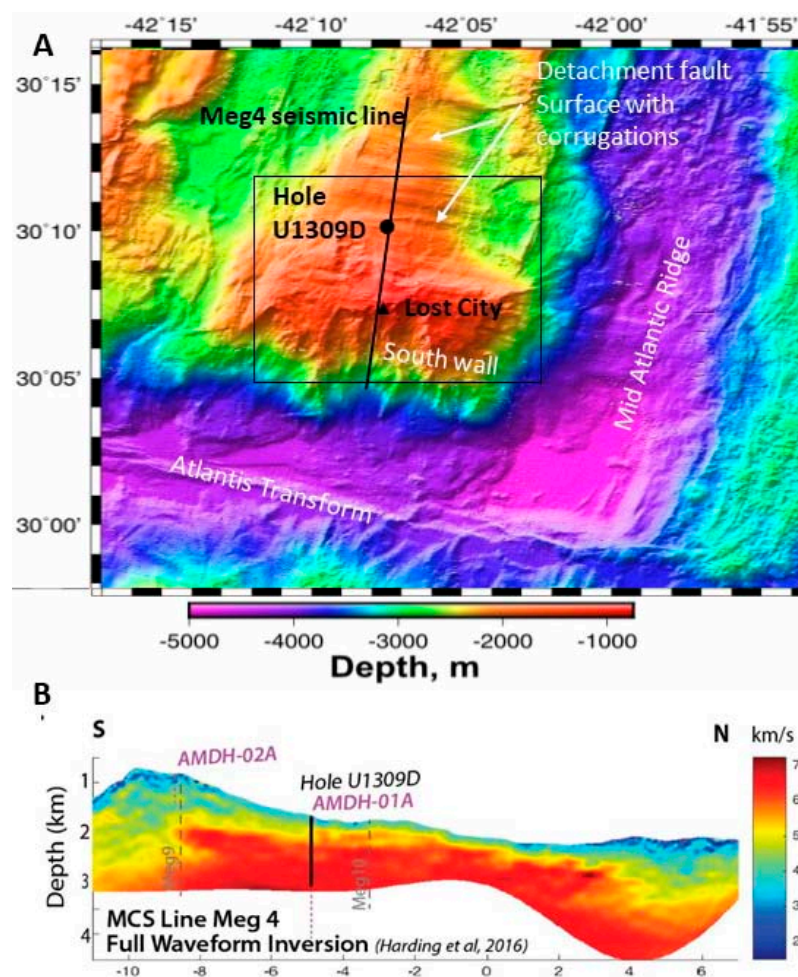


Figure F2. A. Atlantis Massif showing main structural features, location of LCHF, and Hole U1309D. Bathymetry was collected during Expedition 357 (Früh-Green et al., 2018; Escartín et al., 2022). Box = area of Figure F3. B. Full waveform inversion of Seismic Line Meg 4 and locations of proposed primary Sites AMDH-01A (Site U1309) and AMDH-02A. Modified after Harding et al. (2016).

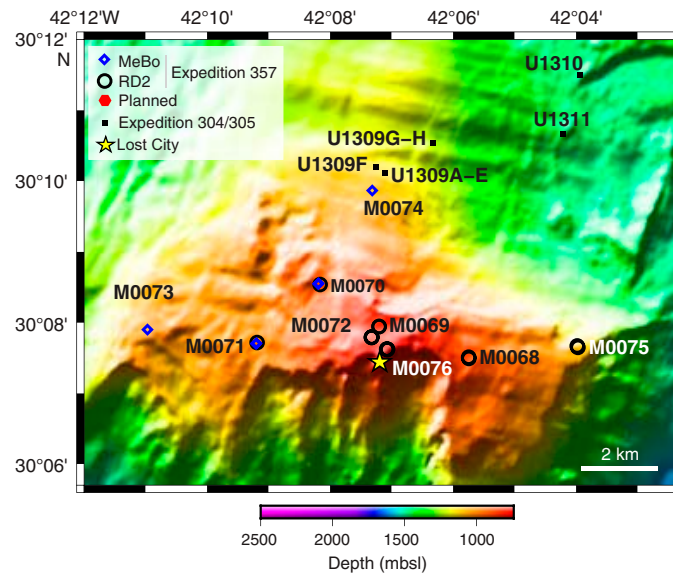


Figure F3. Location of previous drilling during Expeditions 304/305 and 357 (modified after Früh-Green et al., 2016). MeBo = Meeresboden-Bohrgerät 200 drill, RD2 = RockDrill2 drill. Expedition 399 primary sites are at Site U1309 (proposed Site AMDH-01A) and between Sites M0069 and M0072 (proposed Site AMDH-02A).

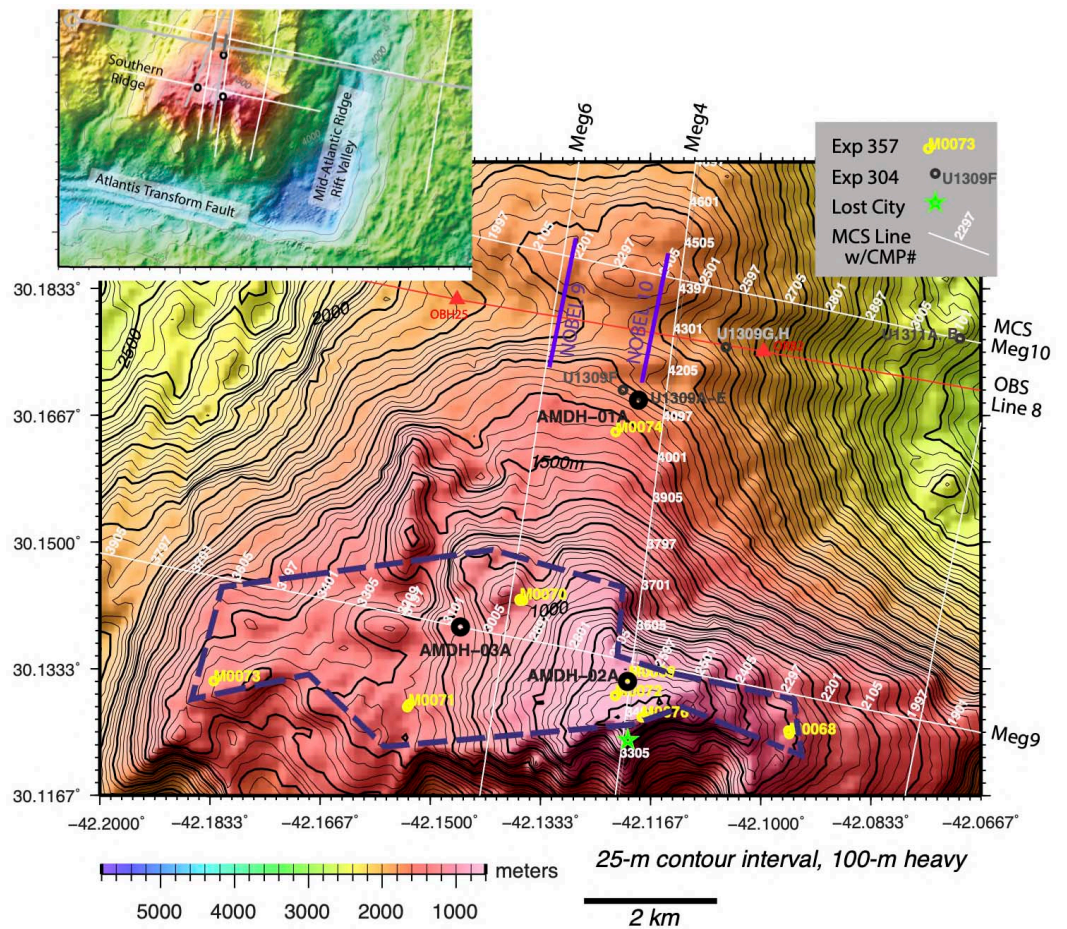


Figure F4. Summary of new sites proposed for Expedition 399. Dashed polygon = area representing Site AMDH-05A, contained within rectangle approved for safety purposes (Figure F1). A series of single-bit holes would be drilled if operations at primary Sites AMDH-01A and AMDH-02A and main alternate Site AMDH-03A fail. (Note that Site AMDH-04A is from early version of proposal and was removed). Previous drill sites (Figure F3) shown for reference. CMP = common midpoint. Taken from Proposal 937-Add.

Hole U1309D in the central dome of the massif penetrated largely gabbroic rocks to 1415 meters below seafloor (mbsf) (Figures F2, F3, F4, F5, F6). This site contrasts with the southern wall of the massif near the LCHF, which consists dominantly of serpentinized peridotite with ~20% gabbroic rocks (Figures F2, F5, F7), and was extensively sampled in the upper few meters during Expedition 357 (Früh-Green et al., 2018; Schroeder and John, 2004; Karson et al., 2006). The fault zone comprises talc-tremolite-chlorite schists overprinting serpentinite, with fault breccias and cataclasites locally overprinting higher temperature fault rocks including amphibolites, gabbros, and syntectonic diabase dikes intruded in the fault zone (Blackman et al., 2011; McCaig et al., 2010; McCaig and Harris, 2012).

During Expedition 399, we plan to revisit Hole U1309D in the central dome of the massif and also attempt shallow (~200 m) coring in a new hole (proposed Site AMDH-02A) near Expedition 357 Hole M0069A within the footprint of Expedition 357 on the southern wall (Figures F2, F3, F4, F5). An additional single-bit hole will be drilled at proposed Site AMDH-01A (Site U1309), targeting reaction porosity in gabbro and diabase, which we hypothesize to be a potential vector for high microbiology cell counts.

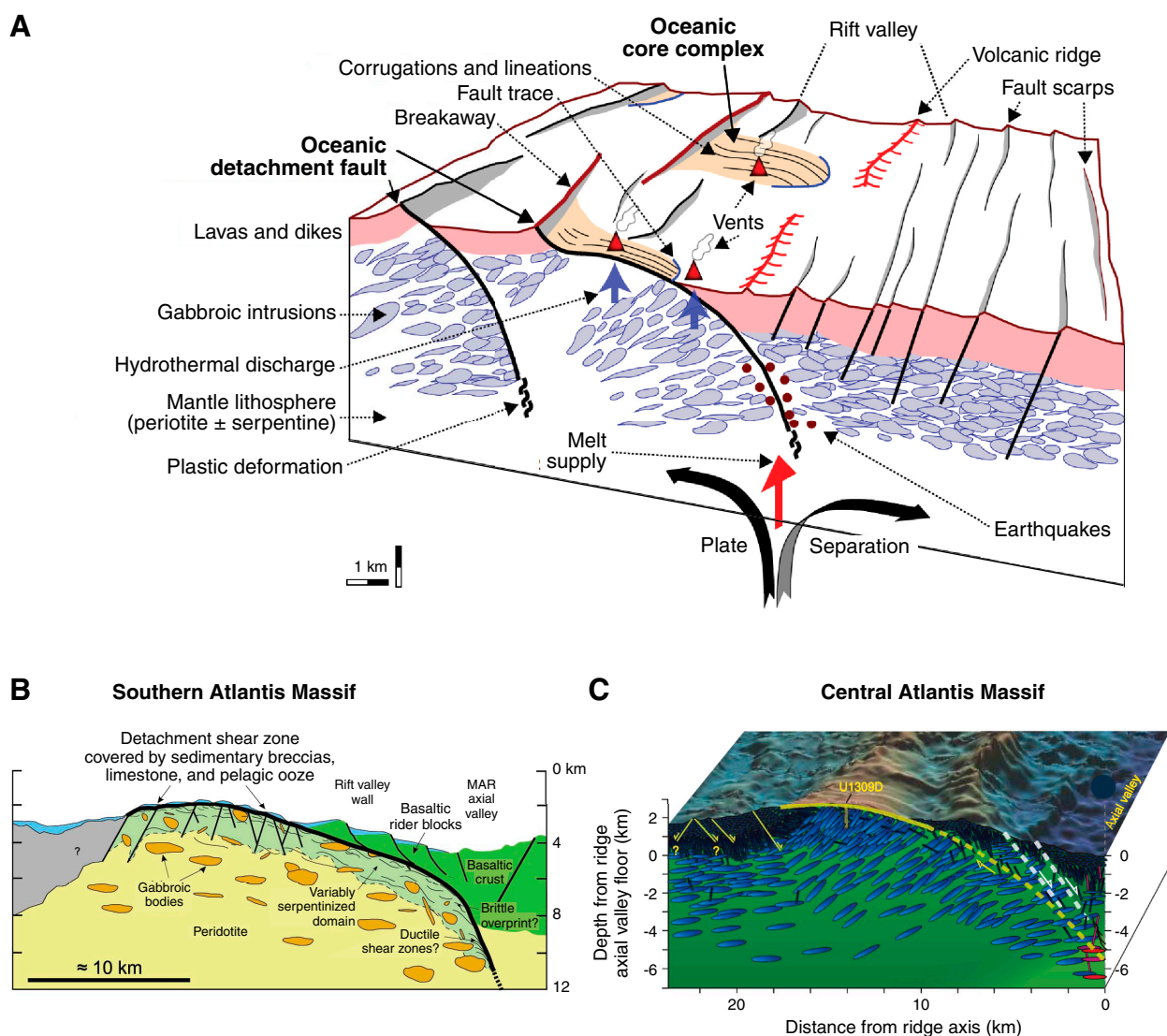


Figure F5. Conceptual sketches of tectonomagmatic evolution of heterogeneous lithosphere and denudation of mantle rocks as detachment faulting progresses (Früh-Green et al., 2016). A. Generic “detachment mode” seafloor (Escartin and Canales, 2011). B. Southern wall of Atlantis Massif is dominated by variably altered peridotites with gabbroic lenses (Boschi et al., 2006). 100 m thick detachment fault zone containing talc-tremolite-chlorite metasomatic schists is at the summit (Karson et al., 2006). MAR = Mid-Atlantic Ridge. C. In contrast, major gabbroic intrusions dominate the central dome (Grimes et al., 2008).

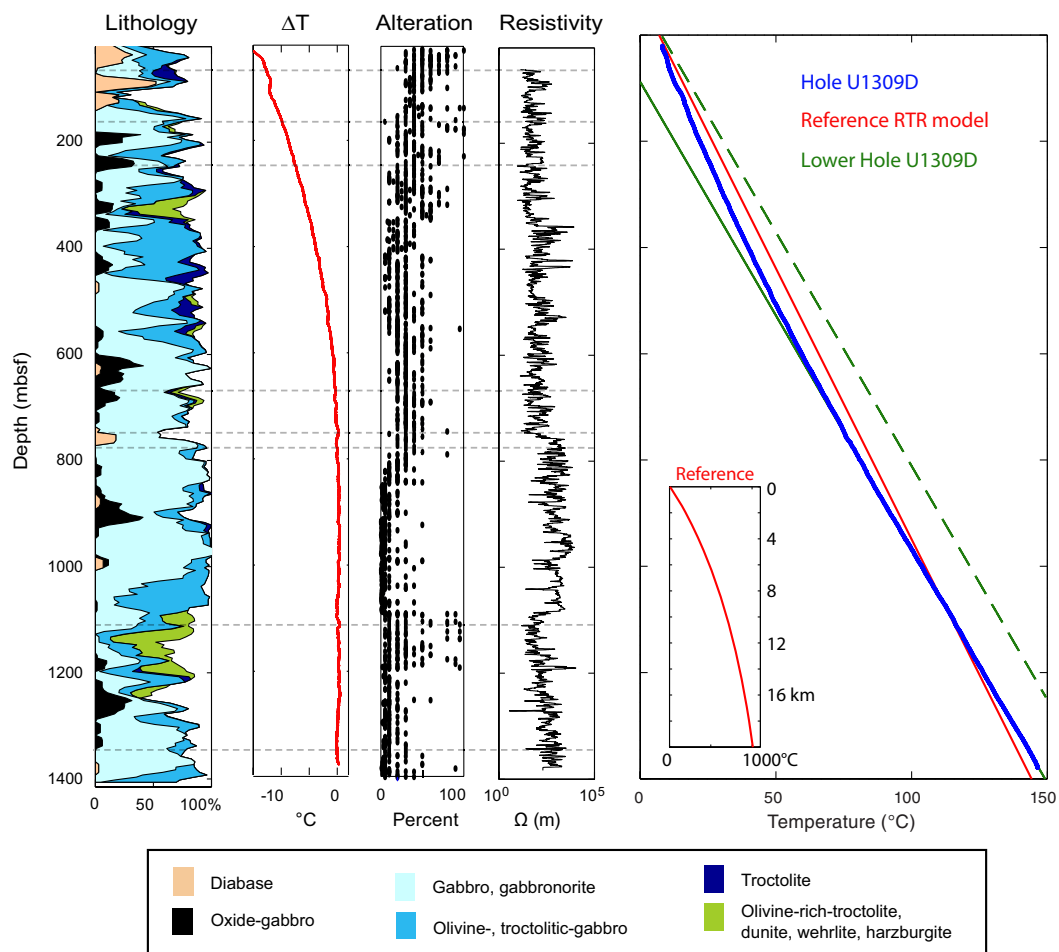


Figure F6. Lithology, temperature, and resistivity logging results, Expeditions 304/305 and 340T and Hole U1309D (after Blackman et al., 2014). ΔT = difference between observed temperature and an extrapolation of conductive gradient at depth to the surface. Minor excursions in temperature are interpreted to be zones of fluid flow at 746 mbsf, where temperature gradient changes from convective to conductive, and 1107 mbsf, near a zone of olivine-rich troctolite.

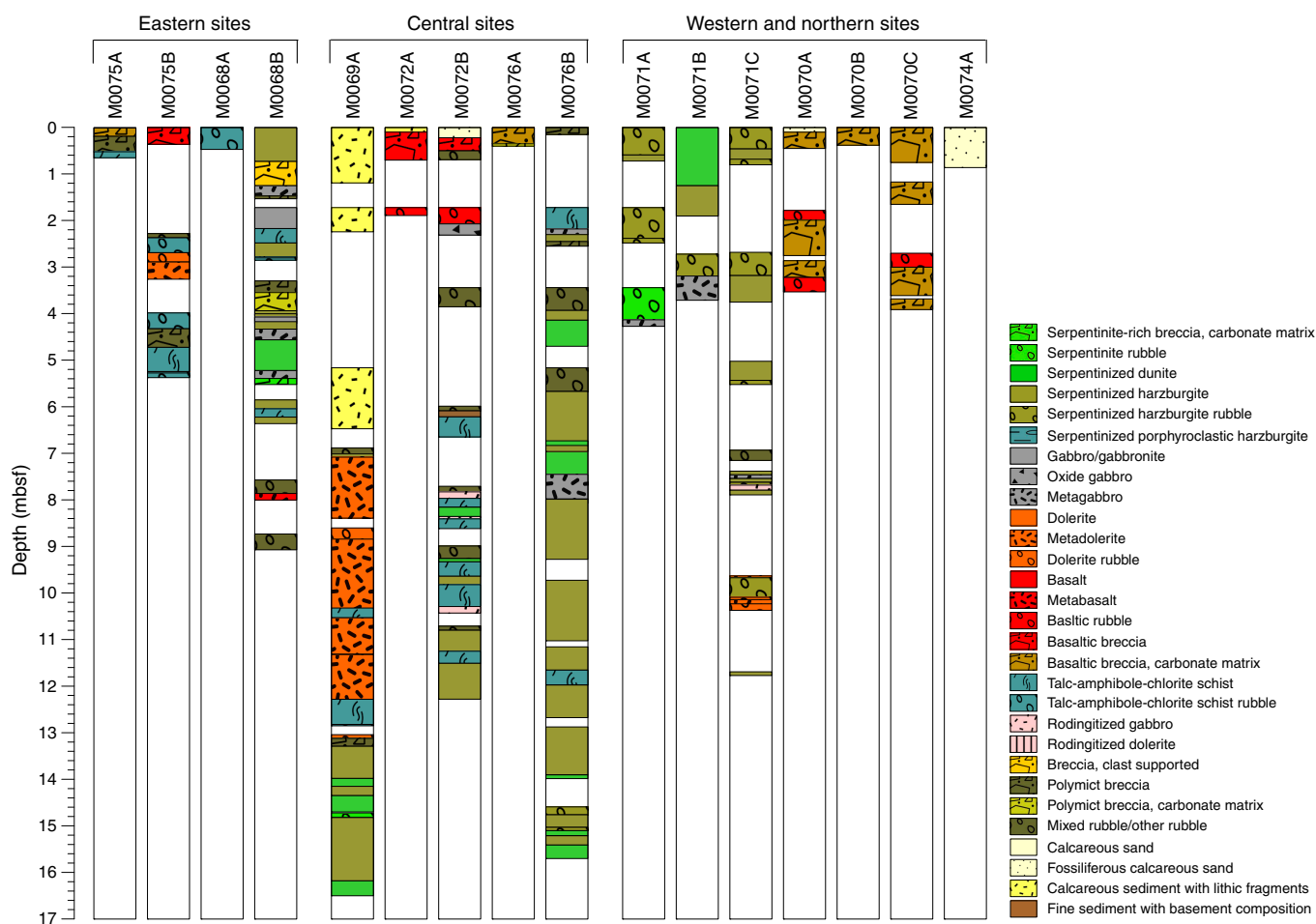


Figure F7. Lithologic summaries from Expedition 357 holes along southern wall of Atlantis Massif (from Früh-Green et al., 2016, 2018). Proposed primary southern wall Site AMDH-02A is close to Hole M0069B, where metadolerite (metadiabase) intrudes into talc-tremolite-chlorite schists, which are brecciated and underlain by a subhorizontal brittle fault zone at ~13 mbsf. Below this fault are little-deformed serpentinized harzburgite and dunite. Beneath the soft-sediment layer, hole recovery was excellent.

3. Background

3.1. Geologic setting and previous work

The Atlantis Massif is an inside corner high on the right-stepping, sinistral, Atlantis I transform fault at 30°N on the Mid-Atlantic Ridge (Figure F2). The massif formed within the last 1.5–2 My. It was the first corrugated massif identified as an OCC (Cann et al., 1997), and it is capped by a domal detachment fault with corrugations parallel to the spreading direction (Figure F5). To the east, the detachment surface disappears beneath a hanging wall composed of fresh basaltic rocks, and is truncated by steep east facing median valley faults. Recent interpretations (Escartín et al., 2022) suggest that a relic of the detachment fault has been trapped in the bottom of the axial valley by a westward ridge jump. To the west, a breakaway is assumed to be present but has never been unequivocally located. The shallowest part of the massif is at the top of the south wall, with a depth <700 meters below sea level (mbsl), and the detachment fault slopes north toward the central massif, where Site U1309 is located. To the north, the detachment is inferred to disappear beneath fault blocks of basaltic rock.

Early work on the massif concentrated on dredging and submersible studies of the south wall (Figure F5B), which is dominated by serpentinized peridotite with inclusions of gabbro (Cann et al., 1997; Blackman et al., 1998, 2002). This slope is a transform fault wall degraded by slope failure, and it forms the footwall of the LCHF (Kelley et al., 2001, 2005). Geophysical surveys include a

refraction experiment (Detrick and Collins, 1998) and multichannel seismic (MCS) profiles (Canales et al., 2004). High velocities were inferred from the refraction data and interpreted to be fresh peridotite at quite shallow depths. However, Hole U1309D (drilled during Expeditions 304 and 305 in 2004 and 2005) showed that the central massif was floored predominantly by gabbro to at least 1415 mbsf (Figures F5, F6), requiring reevaluation of the internal structure of the Atlantis Massif and the geophysical interpretation. Canales et al. (2008) reprocessed the MCS data in terms of *P*-wave tomography, showing high velocities in the central massif and lower velocities under the South Ridge, with a steep contact between a gabbroic domain and a serpentinite domain to the south. Further processing of the MCS data by Henig et al. (2012) improved the resolution of the imaging, and full waveform inversion (Figure F2B) by Harding et al. (2016) produced sharper and more detailed images, groundtruthed by the deep Hole U1309D (Figure F6). It remains very difficult to resolve variably serpentinized peridotite from variably altered gabbro beneath the South Ridge, but an irregular intrusive contact between gabbro and partially serpentinized peridotite seems most likely.

Hole U1309D was revisited during Expedition 340T (Blackman et al., 2013, 2014), which carried out an extensive wireline logging program, including a vertical seismic profile and a temperature profile. The temperature gradient proved to be nearly linear below 750 mbsf, indicating a conductive thermal gradient in the lower part of the hole.

Expedition 357 was a mission-specific platform expedition during which a series of shallow holes were drilled (to a maximum of 16.4 mbsf) in the southern part of the massif using seabed drills (Figures F2, F3, F4, F7) (Früh-Green et al., 2017, 2018). Excellent sections were collected through fault rocks and alteration zones, complementing the data from Site U1309. However, the aim of reaching 80 mbsf was not achieved.

3.2. Igneous petrology

Rocks recovered from Hole U1309D include a sequence of primitive gabbro and olivine gabbro (Figures F6, F8) with intervals of troctolite and olivine-rich troctolite and several diabase intrusions in the uppermost 100 m of the hole. Back-correcting for rotation, the diabase intrusions in the detachment zone could represent a lateral dike–gabbro transition (McCaig and Harris, 2012). Olivine-rich troctolites are interpreted to be mantle rocks modified by melt-rock reaction (Drouin et al., 2009; Ferrando et al., 2018; Lissenberg and MacLeod, 2017); less modified mantle rocks are confined to very short intervals (<1 m) at shallow depths. The gabbro contains many internal contacts (Suhr et al., 2008) and local igneous layering. Plutonic rocks recovered from Hole U1309D are amongst the most primitive ever recovered (Figure F8). Unlike other drilled plutonic sections (Pacific Ocean: Deep Sea Drilling Project [DSDP] Hole 147 and Ocean Drilling Program [ODP] Hole 1256D; Indian Ocean: ODP Holes 735B and 1105A and IODP Hole U1473A), many of the Atlantis Massif plutonic rocks are in equilibrium with mid-ocean-ridge basalt (MORB), with some primitive enough to have formed directly from primary mantle melts. Hence, the Atlantis Massif offers a unique opportunity to study the compositions of melts delivered to the crust from their mantle source and how they evolve to MORB. This is paramount; crustal evolution of melt is now recognized to be significantly more complicated than previously realized, involving not only fractional crystallization but also in situ crystallization and reactive porous flow (Lissenberg and MacLeod, 2017). Hence, interpreting MORB compositions and implications for the upper mantle is highly nonunique, unless melt evolution processes in the lower crust are quantified.

Intervals of gabbro in south wall serpentinites (Figure F5) have an uncertain relationship to the main gabbro farther north but also show evidence of melt-rock reaction (Whattam et al., 2022). They may be intrusions of different age or level of exhumation, or they may be satellites of the larger body. Establishing the genetic relationship between these bodies is important.

3.3. Structural and alteration history of the massif

The Hole U1309D section is remarkable for the paucity of high-temperature crystal-plastic fabrics compared to the only other deep OCC holes at Atlantis Bank (Dick et al., 2017; Ildfonse et al., 2007; McCaig et al., 2010). However, significant breccia intervals occur in the uppermost 100 m of Holes U1309B and U1309D (Blackman et al., 2011). These both deform and are cut by syntectonic

diabase (dolerite) intrusions common in the same interval (Figures F3, F7). Brecciation is inferred to have occurred over a wide range of temperatures up to near magmatic (McCaig and Harris, 2012). Alteration is pervasive in the upper part of Hole U1309D, and isotopic data shows the detachment fault zone to be highly altered by seawater-derived fluids at temperatures similar to black smoker fluids (McCaig et al., 2010). Greater intensities of crystal-plastic deformation were found in gabbroic lenses in peridotite on the south wall of the massif (Schroeder and John, 2004) and in the shallow cores from Expedition 357 (Früh-Green et al., 2018).

Intense alteration in the shallow Expedition 357 cores (Früh-Green et al., 2018; Rouméjon et al., 2019) is generally consistent with previous work on the south wall (Boschi et al., 2006). Early serpentine replacing olivine is locally overprinted by talc-tremolite-chlorite assemblages often associated with mafic intrusions and/or shearing. Carbonate veining is surprisingly rare and almost exclusively observed at the drill sites closest to the LCHF (Ternieten et al., 2021). Extensive water-rock interaction at variable temperatures is further reflected in heterogeneous sulfur isotope compositions (Liebmann et al., 2018). These document a complex evolution of the hydrothermal system with episodes of low-temperature serpentinization and incorporation of seawater sulfate facilitating microbial activity and episodes of high-temperature water-rock interaction controlled by the intrusion of microgabbroic veins, which is accompanied by considerable mass transfer.

Alteration in Hole U1309D records progressive fluid influx during cooling from magmatic to ambient temperatures. It is pervasive above 300 mbsf, with olivine-plagioclase corona reactions reflecting temperatures above 500°C (Nozaka and Fryer, 2011). Deeper, the corona reaction is restricted to the vicinity of fault zones and lithologic contacts, but partial serpentinization of olivine is common in many intervals and often accompanied by prehnite and hydrogarnet replacing plagioclase (Frost et al., 2008). Serpentinization reactions are complex, including early brucite-antigorite veins followed by lizardite-magnetite (Beard et al., 2009). Lower temperature serpentine is often accompanied by saponite (Nozaka et al., 2008), and this has recently been shown to contain abiogenic amino acids (Ménez et al., 2018). Sr and O isotope alteration by seawater-derived fluids is common in the upper part of the hole but decreases below 350 mbsf and is mainly present in serpentine-rich intervals where the primary Sr content is low and the seawater signal may be carried by carbonates (McCaig et al., 2010).

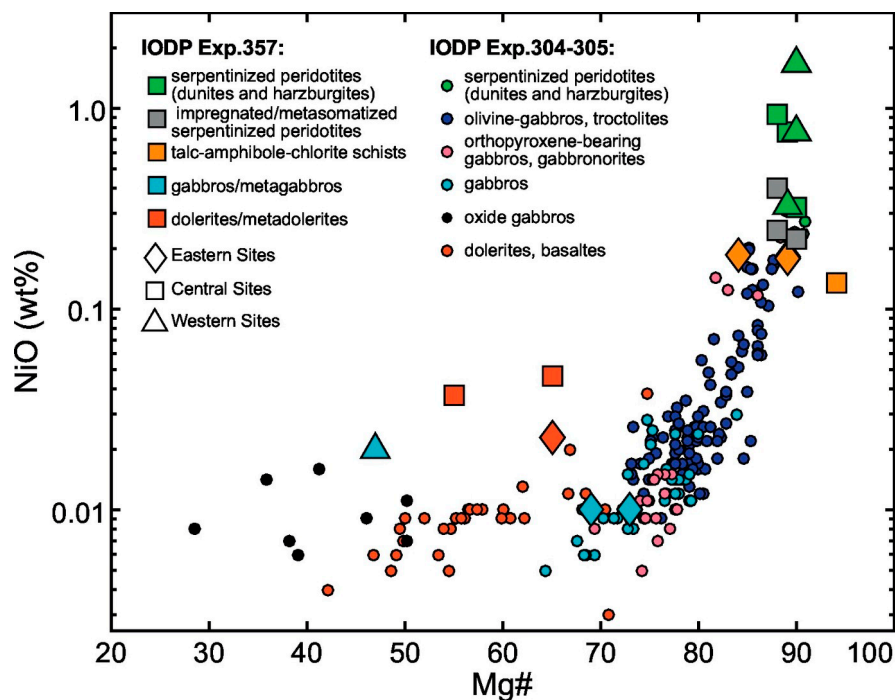


Figure F8. Summary of igneous compositions, Hole U1309D (Expedition 304/305; Godard et al., 2009) and Expedition 357 core samples (from Früh-Green et al., 2018). Note very primitive compositions of many of the gabbroic rocks compared to the diabase (dolerite) dikes, which are similar to MORB at 30°N in the Atlantic.

Reaction permeability is common in the upper part of Holes U1309B and U1309D and has been found in chloritized gabbros in Expedition 357 cores (Figure F9). Rapid dissolution of primary minerals can occur if far from equilibrium hot fluid is in excess, as is likely in the upflow zone of a black smoker system (Cann et al., 2015).

Initial cooling of the massif was rapid, based on paleomagnetic (Morris et al., 2009) and geochronological (Grimes et al., 2008; Schoolmeesters et al., 2012) data. This may have been linked to circulation of black smoker fluids in the detachment fault zone (McCaig et al., 2010; McCaig and Harris, 2012) in an early phase of circulation compared to the current Lost City phase.

3.4. Present day thermal structure and hydrothermal circulation

Expedition 340T (Blackman et al., 2014) found that the temperature profile in Hole U1309D was conductive below 750 mbsf, with a gentle curvature suggesting slow downflow of fluid above that depth (Figure F6). Minor excursions in downhole temperature at 750 and 1100 mbsf suggest fluid influx into permeable fault zones. To vent at up to 90°C, the LCHF must mine fluid to several kilometers depth, based on inferences of circulation temperatures from fluid chemistry (Kelley et al., 2005; Allen and Seyfried, 2004, 2005; Foustoukos et al., 2008) and hydrothermal modeling (Titarenko and McCaig, 2016; Lowell, 2017). At high levels, the LCHF is localized by faulting (Denny et al., 2016); whether more diffuse or multichannel flow occurs at depth or whether there is shallow recharge and mixing is very important for the chemical and hence microbiological evolution of the system and therefore underpins all of our main objectives. The LCHF may be driven in part by exothermic serpentinization reactions (Früh-Green et al., 2004), but this is not certain because a lateral permeability change could stabilize and sustain the LCHF over long periods of time (Titarenko and McCaig, 2016). New measurements of the thermal structure and fluid flow at depth in proposed Hole AMDH-02A close to Lost City will provide important constraints on the hydrogeology of the Atlantis Massif.

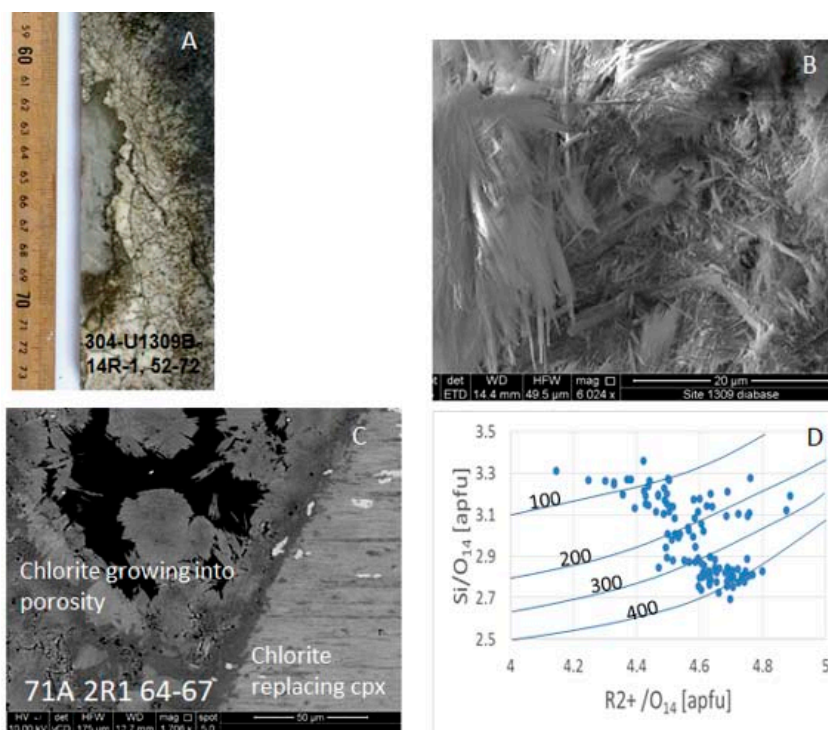


Figure F9. Reaction porosity in Atlantis Massif. A. Amphibole filled vug in gabbro with bleached reaction rim of sodic feldspar and minor amphibole at 72 mbsf, Hole U1309B. Relic porosity is common both in the vug and the reaction rim. Vug is interpreted to be a section through a stockwork pipe for black smoker fluids flowing up the detachment fault. B. Fibrous amphibole filling porosity formed by dissolution of clinopyroxene (cpx) in diabase (dolerite), Hole U1309B. C. Chloritized gabbro with plagioclase completely dissolved and the space filled by chlorite, Hole M0071A. D. Chlorite geothermometry (Bourdelle and Cathelineau, 2015) showing that the vugs filled over a temperature range of 400° to <100°C.

3.5. Potential for abiotic organic synthesis

It is axiomatic that before life could begin on Earth or other worlds in the solar system, precursors of DNA, RNA, proteins, and other biologically relevant macromolecules must have been synthesized without biological intervention (Stüeken et al., 2013). The LCHF and Atlantis Massif have many features that make these synthesis reactions favorable; these locations have therefore been proposed as a model for the early Earth settings where prebiotic chemistry may have led to life (Kelley et al., 2002; Martin et al., 2008). Serpentinization and abiotic organic synthesis reactions play a major role in generating H₂ and organic carbon molecules that are carried with fluids, including methane, ethane, propane, and small carboxylic acids such as formate (Kelley et al., 2001, 2005; Proskurowski et al., 2008; Lang et al., 2010, 2018; Wang et al., 2018; Klein et al., 2019). In samples recovered from nearby Hole U1309D, the amino acid tryptophan and additional carbonaceous material have been identified in association with iron-rich saponitic clays and proposed to be synthesized abiotically (Pisapia et al., 2018; Ménez et al., 2018).

A major driving factor for organic synthesis reactions is the production of H₂ in association with serpentinization reactions, which makes the reduction of CO₂ thermodynamically favorable (McCollom and Seewald, 2013). H₂ is likely to be generated from the reduction of H₂O circumstances where the average Fe³⁺/Fe²⁺ of secondary minerals is higher than that of primary minerals (Andreani et al., 2013; McCollom and Bach, 2009), although experiments suggest generation rates are highest around 300°C (McCollom et al., 2016). Hydrogen has been detected in the water column widely across the Atlantis Massif, even in locations not associated with the focused circulation pathway of the LCHF (Lang et al., 2021).

Temperature and lithology are likely major controls on the type and abundance of organic compounds synthesized at the Atlantis Massif. Some reduced compounds, such as methane and short-chain alkanes, are believed to form through Fischer-Tropsch-type reactions at temperatures well above the known limit to life (Proskurowski et al., 2008; Wang et al., 2018; Klein et al., 2019), perhaps catalyzed by Fe-, Ni-, and Cr-bearing minerals (Foustoukos and Seyfried, 2004). These compounds may form at high temperature, trapped in fluid inclusions, and be mobilized into circulating fluids when the system is at lower temperatures (Kelley and Früh-Green, 1999, 2001; Klein et al., 2019). In contrast, the formation of carboxylic acids, amino acids, and carbonaceous material likely proceeds at lower temperatures (<400°C), including within thermal regimes conducive to life (McDermott et al., 2015; Lang et al., 2018; Ménez et al., 2018; Klein et al., 2019).

Expedition 399 coring will enable examination of abiotic organic synthesis in multiple settings spanning distinct thermal and geochemical regimes. First, deepening Hole U1309D will result in core material that has never experienced temperatures lower than 140°C, except during the brief period of sample collection and recovery, allowing examination of organic formation beyond the known thermal limit for life. Second, proposed Site AMDH-02A will result in up to 200 m of core from the actively serpentinizing southern wall of the massif. In addition to recovering core material, complementary fluid samples will be collected from down the boreholes. Recovered samples will provide an opportunity to link the variations in physicochemical conditions to the diversity of organic molecules and synthesis reactions identified in solid and fluid substrates. Pore fluids may also be recovered from samples containing reaction porosity both in the serpentine-rich environment of proposed Site AMDH-02A and the gabbroic environment of proposed Site AMDH-01A.

3.6. Examining the thermal limits of life and the deep biosphere in oceanic crust

To date, there is very little information about the existence of a deep biosphere in seafloor serpentinizing systems. The warmest, highest pH domains of carbonate chimneys from the LCHF are dominated by a single clade of Lost City Methanosarcinales (Schrenk et al., 2004). Chimney exteriors are mixing zones between seawater and anoxic alkaline fluids and create gradients conducive to biochemical and microbial activity (Summit and Baross, 2001; McCollom and Seewald, 2007; Lang and Brazelton, 2020). DNA sequencing and lipid biomarker analyses have identified communities involved in H₂, CH₄, and sulfur cycling (Bradley et al., 2009; Brazelton and Baross, 2010; Brazelton et al., 2010, 2006; Méhay et al., 2013). A portion of the community actively cycles for-

mate, an organic acid formed abiotically deep in the circulation pathway (Lang et al., 2018; McGonigle et al., 2020).

Prior to Expedition 357, it was hypothesized that subsurface mixing zones between hydrothermal fluids and seawater, together with organic rich zones related to serpentinization, would lead to a diverse ecosystem that includes both chemolithotrophs and heterotrophs (Früh-Green et al., 2015). It was also hypothesized that serpentinizing environments would sustain higher biomass than gabbro-dominated domains such as that sampled in Hole U1309D, where cell counts were below detection limit but gene sequencing revealed evidence for bacteria largely related to hydrocarbon degraders (Mason et al., 2010).

Microbial cell abundances in the shallow Expedition 357 core samples were variable and relatively low, ranging from tens to thousands of cells per cubic centimeter (Früh-Green et al., 2018); many of the samples were below the minimum quantification limit of 9.8 cells/cm³ (Figure F10). The deepest serpentinite samples from Expedition 357 Holes M0072B (6.5 mbsf) and M0069A (14.6 mbsf), sites closest to the LCHF (Figure F3), have cell densities of 10–24 cells/cm³ (Früh-Green et al., 2018). These cell densities are distinctly lower than in the actively venting LCHF carbonate towers (10⁷–10⁸ per gram of wet weight (Kelley et al., 2005). They are also low in comparison to cell densities in fluids sampled in actively serpentinizing environments on land, which are typically less than 10⁵ cells/mL and as low as 10² cells/mL, although such locations represent different niches in the subsurface ecosystem (e.g., Brazelton et al., 2017; Schrenk et al., 2013). These cell densities are also lower than in mafic subsurface cores, which have been estimated at ~10⁴ cells per gram of rock (Jørgensen and Zhao, 2016). Overall, this low density suggests that something may be limiting life in this subsurface habitat compared to the other habitats, such as high pH, low carbon dioxide availability, or low solvent access owing to low porosity (Lang and Brazelton, 2020), but further analyses and additional samples are required to determine this.

Insights to the constraints on life in the subsurface and the metabolic strategies that the small numbers of inhabitants employ can be gained in part through characterization of the endolithic communities. Distinguishing endemic microbial taxa from those introduced from seawater or contamination is a major challenge requiring multiple strategies to overcome (Kallmeyer et al., 2017; Sylvan et al., 2021; Pendleton et al., 2021). Nonetheless, the signatures of endolithic commu-

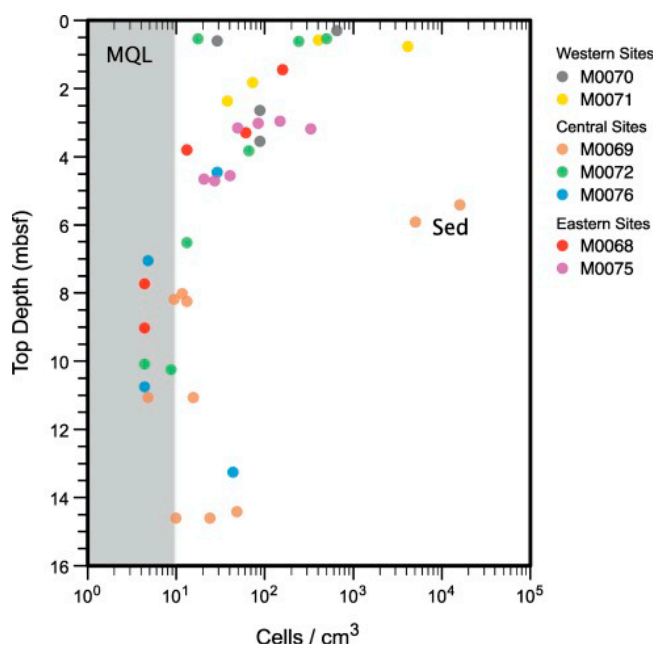


Figure F10. Cell counts from interior portions of whole-round cores, Expedition 357. Shaded area = minimum quantification limit (MQL) of 9.8 cells/cm³. Sediment (Sed) samples from Site M0069 have higher cell counts than other samples from similar depths. Cell counts are generally low; serpentinites at the base of Hole M0069A are the deepest samples with significant cell counts. From Früh-Green et al. (2018).

4. Scientific objectives

Operations during Expedition 399 should allow us to address the following objectives.

4.1. Objective 1: characterizing the life cycle of an oceanic core complex and the links among igneous, metamorphic, structural and fluid flow processes

4.1.1. Scientific rationale

The Atlantis Massif is probably the best studied near-ridge site in the ocean floor; this allows our objectives to be driven by process and hypothesis rather than exploration. At the end of the expedition, we will have collected important new data on both ancient processes during deformation and alteration of the detachment fault rocks and the underlying massif and on the current thermal and hydrological structure of the massif and ongoing processes of fluid-rock interaction. We will have collected the first complete section through an oceanic detachment fault in serpentinites, complementing the shallow holes cored during Expedition 357 and will have collected the first IODP samples in a stable ocean crust regime with ambient temperatures ranging up to 220°C.

We will study the evolution of the Atlantis Massif by deepening Hole U1309D to ~2060 mbsf, accessing ambient temperatures from 147° to ~220°C, and by drilling a new 200 m deep hole in serpentinite containing gabbro and mafic dikes close to the LCHF.

4.1.2. Expected outcomes

We expect the following outcomes:

- In Hole U1309D, borehole fluids collected at temperatures up to 145°C will be analyzed for a full suite of major and minor elements and isotopes, including reactive elements such as boron, particularly above and below zones of suspected fluid ingress into Hole U1309D. Comparison with wall rock lithologies will allow rates of fluid-rock reaction since Expedition 340T in February 2012 to be estimated. The deepened hole will be open for future fluid sampling up to 220°C.
- Rock samples, forming part of the longest continuous section through young gabbroic crust to date in Hole U1309D, will allow the study of igneous and alteration processes in rocks that have never been below 140°C (other than briefly during drilling).
- A complete section from 15 to 200 mbsf will be drilled through the oceanic detachment fault zone in serpentinitized ultramafic rocks at proposed Site AMDH-02A and into less deformed rocks below. Core information will be complemented by logging and paleomagnetic data for full structural reorientation. Temperature measurements will allow improved modeling of LCHF circulation.
- A new 80 m deep hole at proposed Site AMDH-01A in the vicinity of Hole U1309D will allow the calculation of the average strike and dip of diabase intrusions already correlated between Holes U1309B and U1309D.

Drilling will allow us to test the following specific hypotheses:

- The proportion of ultramafic rock will increase as Hole U1309D is deepened, reflecting a gradual transition into mantle rocks. Much of both the main gabbro and smaller bodies in proposed Hole AMDH-02A are expected to show evidence of assembly by melt-rock reaction rather than discrete intrusion.
- Reaction porosity will be found on the margins of gabbroic intervals in contact with ultramafics (blackwall zones) in the detachment fault zone and will yield formation waters distinct from Lost City vent fluids because of isolation from the main flow system.
- Deformation in the south wall fault zone will be multistrand, and strain will not be focused into shearing of serpentine but rather into tremolite-rich assemblages as seen in the cores from Expedition 357.
- Isotopically heavy seawater-derived boron will not be present in the deep section of Hole U1309D and may die out with depth at proposed Site AMDH-02A. Boron profiles will allow a

better estimate of the boron content of slow-spread crust to be made than those based on near-surface collected samples.

4.2. Objective 2: accessing the chemical kitchen that preceded the appearance of life on Earth

4.2.1. Scientific justification

A consensus is emerging that abiotic serpentinization related reactions play a major role in generating H_2 and various forms of organic compounds (Kelley and Früh-Green, 1999; Proskurowski et al., 2008; McCollom and Bach, 2009; McCollom and Seewald, 2013, Klein et al., 2013, 2019; Lang et al., 2010, 2018; McDermott et al., 2015; McCaig et al., 2020). These compounds can become mobilized and available for microbial activity at lower temperatures around vent systems such as the LCHF, potentially the type of location where life evolved on the early Earth (Kelley et al., 2002). An open question is what the rates of serpentinization, hydrogen generation, and organic synthesis may be. We aim to identify chemical gradients in both H_2 and organic compounds and other associated components to allow modeling of reaction rates. In situ observations in core will give control information on what compounds, both organic and inorganic, are actually produced in association with varying temperatures and lithologies.

Both the deepened Hole U1309D and the new hole at proposed Site AMDH-02A hosted in peridotites will be left such that they can be relogged for fluid chemistry and temperature in the future, allowing for estimates of the rates of other fluid-rock reactions at various temperatures or possible ingress of formation waters.

4.2.2. Expected outcomes

We will sample organic molecules and H_2 in fluid inclusions, core material, sedimentary pore waters, and borehole fluids in both the deepened Hole U1309D and the new hole at proposed Site AMDH-02A. The recovery of material from diverse lithologies and thermal regimes will provide the following opportunities:

- To sample rocks of variable lithology over a temperature range of 147°–220°C from 1414 to ~2060 mbsf in Hole U1309D; at these temperatures, H_2 production should proceed readily and recovered rocks would have been at temperatures above that of the limit for life throughout their geological history; abiotic organic synthesis reactions at these temperatures could favor more reduced types of molecules such as methane and hydrocarbons over more oxidized compounds such as organic acids and amino acids;
- To sample fluids in existing Hole U1309D in a range of lithologies and locations where fluid ingress is suspected and at temperatures up to 140°C;
- To identify the distribution of H_2 and CH_4 with depth, temperature, and lithology;
- To assess the potential for further H_2 generation by systematic measurement of Fe^{3+}/Fe^{2+} ratios of secondary and primary assemblages;
- To sample lower temperature rocks at proposed Site AMDH-02A that are likely more suitable for the abiotic formation of a more diverse suite of organic molecules including formate, acetate, and amino acids; we will seek these compounds in formation waters contained in reaction porosity and other permeable zones such as dike margins and fault rocks along with borehole fluids;
- To constrain the availability and form of inorganic carbon that could be used as a starting material for abiotic synthesis reactions; and
- To identify the association of organic molecules with alteration phases such as clays.

Drilling will allow us to test the following specific hypotheses:

- Generation of H_2 is widespread, it is abundant in fluid inclusions and borehole fluids associated with ultramafic lithologies, and the highest concentrations are associated with higher temperatures.
- Generation of CH_4 occurs primarily at high temperatures and in many cases has already been formed and trapped. In lower temperature settings, it is released from the rock into circulating fluids.

- Saponite and other iron-bearing minerals whose formation is accompanied by H₂ production (e.g., hydrogarnets) provide rich microsites for abiotic organic synthesis; lithologic contacts and alteration zones generate higher concentrations of more complex compounds due to enhanced chemical disequilibria.
- Carbonate deposition will be higher in the detachment zone accessed by drilling at proposed Site AMDH-02A, in contrast to the relatively sparse veins found on the south wall during Expedition 357.

4.3. Objective 3: characterize the deep biosphere and limits for life in the Atlantis Massif, in particular the impact of lithologic substrate, porosity, permeability, temperature, fluid chemistry, and reactive gradients

4.3.1. Scientific justification

Results from shallow (<16.4 mbsf) coring on the southern wall during Expedition 357 indicate a very low biomass ecosystem (Figure F10) compared to other crustal subsurface systems (Früh-Green et al., 2018). However, this coring did not reach the target depth of 50–80 mbsf, and it is doubtful that any part of the active Lost City flow system was accessed. Sampling did not specifically target the porous and permeable zones most likely to contain more abundant biomass. Reaction porosity in mafic lithologies may increase microbial activity, including lower local pH, nutrient access through permeability, and chemical gradients related to lithologic boundaries and ongoing mineral precipitation (Andreani and Ménez, 2019; Lang and Brazelton, 2020). Operational restrictions during Expedition 357 inhibited the ability to properly characterize the microbiology of serpentinizing seafloor; deeper and more targeted samples are necessary to determine if there are robust depth-, temperature-, or lithology-driven patterns in the abundance or diversity of microbial life and if there are connectivities between this deeper ecosystem and that observed at LCHF. Similarly, sample collection during Expedition 304/305 was not targeted on porous, permeable, and reactive zones (Mason et al., 2010) and may not be representative. Proposed Site AMDH-01A will be drilled to target such zones. Despite low biomass, communities adapted to in situ conditions have been identified in recovered core material, including successful enrichment cultures (Mason et al., 2010; Quéméneur et al., 2019; Motamedi et al., 2020; Goordial et al., 2021).

Sampling for microbiological analyses will specifically target areas of higher porosity and permeability to test whether these regimes are associated with higher cell abundances. The highest cell counts recovered from Expedition 357 were adjacent to highly chloritized gabbro with relict reaction porosity (Figure F9), which was infilled with chlorite down to conditions of <100°C. Increased porosity, a less alkaline local fluid, or chemical gradients between serpentinite and gabbro may have promoted microbial growth. A major aim of drilling at proposed Site AMDH-02A is to recover similar vuggy samples in a more continuous section through the detachment fault zone. Several vugs were found in the uppermost 100 m of Holes U1309B and U1309D (Figure F9A), and smaller scale porosity was found in metadiabase (Figure F9B). This zone will be resampled at proposed Site AMDH-01A.

The thermal structure of the Atlantis Massif offers a unique opportunity to study the temperature limits of a deep life in a crustal system because fluid temperatures in Hole U1309D (Figure F6) are expected to cross both the known upper thermal limit for life in laboratory cultures (122°C) and the lower suspected temperature limit (~80°–90°C) for life in energy-limited subsurface crustal systems (Heuer et al., 2020). Because many portions of the Atlantis Massif seafloor are not energy limited, evidence of active life may be present even at the higher thermal limits only previously reached in laboratory cultures.

4.3.2. Expected outcomes

The samples will provide the following opportunities:

- To link the diversity and abundance of microbial communities with lithology and thermal regime;

- To constrain whether pH, availability of inorganic carbon, or other factors limit life in the subseafloor;
- To determine whether microorganisms are more abundant in regions with porous and permeable zones such as reaction porosity in the edges of gabbroic intrusions, fault rocks, and fractures;
- To determine whether there are common inhabitants in the subseafloor communities despite differences in physicochemical conditions;
- To identify the source(s) of organic carbon consumed by the heterotrophic inhabitants of the subseafloor;
- To isolate microorganisms via enrichment cultures to better understand the growth conditions and physiological requirements of subseafloor life; and
- To evaluate the role of microorganism in mediating exchanges between circulating fluids and the host rock and in accelerating alteration reaction.

Drilling will allow us to test the following specific hypotheses:

- Cell counts higher than previously recovered from the Atlantis Massif (higher than 4×10^3 cells/cm³) will be found in porous and permeable zones such as in reaction porosity at the edges of gabbroic intrusions, fault rocks, and fractures potentially channeling Lost City fluids.
- Higher cell counts and specific types of microbial life will be associated with local fluid chemistry (including H₂, CH₄, organic acids, other organic macromolecules, cation and anion ratios, and if possible pH).
- Heterotrophic metabolisms will be more prevalent than chemoautotrophic metabolisms.
- Evidence for active life will be present up to the thermal limit of life established by laboratory cultures (122°C).

4.4. Connection to the 2013–2023 IODP Science Plan

Expedition 399 will deepen Hole U1309D and drill two new holes on the Atlantis Massif (30°N; Mid-Atlantic Ridge) and will address multiple challenges within the current IODP Science Plan themes Biosphere Frontiers, Earth Connections, and Earth in Motion.

4.4.1. Challenge 5: what are the origin, composition, and global significance of deep subseafloor communities?

To date, there is very little information about the existence of a deep biosphere in subseafloor serpentinizing systems. Results from shallow (<16.4 mbsf) coring on the southern wall of the Atlantis Massif during Expedition 357 indicate a very low biomass ecosystem compared to other crustal subsurface systems, but deeper samples are necessary to determine whether there are robust depth-, temperature-, or lithology-driven patterns in the abundance or diversity of microbial life and whether there are connectivities between this deeper ecosystem and that observed at LCHF. These deeper samples will allow us to characterize the distribution, diversity, and survival strategies of microbial communities in the subseafloor. We will also utilize other signs of life, such as lipid biomarkers, to identify the distribution of relict communities.

4.4.2. Challenge 6: what are the limits of life in the subseafloor realm?

A main hypothesis of Expedition 357 was that serpentinizing environments sustain higher microbial biomass than gabbroic-dominated domains because of the availability of thermodynamic energy from a steady flux of H₂ and abiotic organic molecules (Früh-Green et al., 2015). Instead, the cell counts in the shallow cores across the Atlantis Massif were low in comparison to continental serpentinizing systems and gabbroic systems (Früh-Green et al., 2018), suggesting that a parameter other than energy such as pH, low bioaccessible inorganic carbon, or water availability, limits the biosphere in this subsurface system (Lang and Brazelton, 2020). Quantification of the biomass and rates of microbial activity in cores that span a range of temperatures, geochemical conditions, and porosities will help identify the settings that support biological activity in the subseafloor.

4.4.3. Challenge 9: how are seafloor spreading and mantle melting linked to ocean crustal architecture?

The Atlantis Massif is a key end-member of the process of seafloor spreading, where much of the plate separation is accommodated on a detachment fault (Figure F5). This is in contrast to spreading at fast-spreading ridges where most extension is accommodated by gabbro intrusion, eruption, and diking. The partitioning of strain between faulting and magmatic processes is controversial (Tucholke et al; 2008, Grimes et al., 2008) as is the role of gabbroic intrusions and dikes (Olive et al., 2010; McCaig and Harris, 2012). The extent to which gabbroic rocks are metasomatic products of melt-rock interaction with mantle rocks has also been debated (Drouin et al., 2009; Lissenberg and MacLeod, 2017). Our studies will address all these outstanding issues.

4.4.4. Challenge 10: what are the mechanisms, magnitude, and history of chemical exchanges between the ocean crust and seawater?

Measurement of a wide range of chemical and isotopic components in borehole fluids will be conducted to better understand phase equilibria and fluid-rock interaction processes. Numerous field and experimental studies have demonstrated that dissolved silica, boron, lithium, oxygen, and strontium isotopes, together with redox constraints imposed by dissolved H₂ and coexisting sulfur species, can provide important clues to the role of more deeply seated heat and mass transfer reactions on the chemical evolution of hydrothermal fluids (Allen and Seyfried, 2003; Foustoukos et al., 2008). Data of this sort, for example, can help constrain temperature, fluid/rock mass ratio, and potential sources of silica that may involve alteration of gabbro and/or peridotite lithologies (Bach et al., 2004; Bach and Humphris, 1999; Seyfried et al., 2015; Tutolo et al., 2018). Observations over a range of temperatures from borehole fluid chemical and temperature data will permit assessment of cooling-induced pH changes and B isotope fractionation processes, with insight on the effect of temperature on stable and metastable fluid-mineral equilibria. Deep drilling in Hole U1309D will also allow us to study the uptake of volatile elements such as boron and lithium in rocks that have never been closer than 1.5–2 km from the ocean reservoir. Quantification of Fe³⁺/Fe²⁺ ratios in both fresh and altered samples will allow time-integrated release volumes of H₂ to be calculated, improving and extending existing estimates based on serpentinization to a wider range of rock types. Both holes will remain open for future logging and fluid sampling once thermal equilibrium has returned.

4.4.5. Challenge 13: what properties and processes govern the flow and storage of carbon in the seafloor?

Circulating seawater carries seawater bicarbonate into the subseafloor, whereas crustal processes carry CO₂ from the mantle. Both sources of inorganic carbon can rapidly precipitate as calcium carbonate over a wide range of pressures and temperatures, particularly in association with the alkaline conditions prevalent in ultramafic environments (Frost, 1985; Ternieten et al., 2021). For this reason, serpentinizing environments have been a focus of long-term carbon sequestration programs (Kelemen et al., 2011). The degree to which inorganic carbon remains accessible either in the fluids or in crustal material will have a significant impact on the availability of starting materials for abiotic synthesis reactions and for microbial autotrophy (Lang and Brazelton, 2020). The reduction of inorganic carbon to organic constituents in the absence of biological intervention occurs readily at the Atlantis Massif and LCHF, producing a suite of compounds that includes methane, short-chain hydrocarbons, organic acids, amino acids, and carbonaceous material (Proskurowski et al., 2008; Lang et al., 2010; Ménez et al., 2018; Klein et al., 2019). Expedition 399 will help to constrain the settings in which different types of organic molecules are synthesized as well as the degree to which inorganic carbon is sequestered as carbonate.

4.4.6. Challenge 14: how do fluids link subseafloor tectonic, thermal, and biogeochemical processes?

The thermal structure at proposed Site AMDH-02A will place new constraints on the hydrogeology of the Atlantis Massif, in particular the nature of shallow recharge or discharge in the vicinity of LCHF and the extent to which flow is focused into the current vent field. Fluids in reaction porosity are likely to be trapped “backwater fluids” (Titarenko and McCaig, 2016), perhaps much more rock equilibrated than the rapidly moving LCHF fluids. Such backwater fluids, together with

fluid inclusions (Kelley and Fröh-Green, 1999; Klein et al., 2019) may be the source of components such as H₂ and CH₄ leaking by diffusion into the flow system, and the gradients between slow- and fast-moving fluid regimes with different chemistries may be important for microbial growth (Lang and Brazelton, 2020). In Hole U1309D, we will be able to sample borehole fluids that may have equilibrated for some components with specific lithologies, allowing rates of reaction to be estimated, and gradients of H₂ either in the borehole fluids or fluid inclusions may allow estimation of gas fluxes out of the Atlantis Massif. By deepening Hole U1309D, we hope to approach the temperatures at which H₂ and CH₄ are thought to be generated more rapidly during serpentinization (McCollom et al., 2016). In addition to these present day processes, our profile through the detachment fault zone at proposed Site AMDH-02A will allow the links between deformation, metasomatic alteration, porosity, and permeability generation during deformation at black smoker temperatures and above to be studied and quantified.

4.5. Connection to the 2050 Science Framework

Expedition 399 comes close to the end of the current IODP Science Plan, and it is useful to look forward to the 2050 Science Framework “Exploring Earth by Scientific Ocean Drilling.”

The expedition will contribute to the new Science Framework just as strongly as the current Science Plan, including the Flagship Initiative Exploring Life and its Origins and the following Strategic Objectives:

- Habitability and Life on Earth,
- The Oceanic Life Cycle of Tectonic Plates,
- Feedbacks in the Earth System, and
- Global Cycles of Energy and Matter.

5. Operations plan and coring/wireline logging strategy

Time estimates for the proposed operations are presented in Table T1.

5.1. Proposed Site AMDH-02A

The target area for proposed Site AMDH-02A is a gently sloping region ~50 m from Site M0069 (Figures F2, F3, F4) that gave good recovery of diabase intrusives cutting talc-amphibole-chlorite schist, a brittle fault zone at ~13 mbsf, and undeformed serpentinites to 16.4 mbsf (Figure F7). We plan to occupy proposed Site AMDH-02A twice: at the beginning of operations to drill the hole and a few weeks later to sample fluids and conduct wireline logging after the borehole fluid has partially equilibrated with the formation.

During the first visit to proposed Site AMDH-02A, a camera survey will assess the conditions for drilling. A Niskin bottle will be mounted on the camera frame during every lowering to collect water column samples before and after drilling. An initial pilot hole (Hole A) will be drilled and cored to ~50 mbsf with the rotary core barrel (RCB) system. This will be followed by drilling a hydraulic release tool (HRT) reentry system with 13 $\frac{3}{8}$ inch casing to ~14 mbsf in a second hole (Hole B), which will then be cored with the RCB system to ~200 mbsf. The reentry system will stabilize the upper sections of the hole and allow multiple bits to be run into the hole. During drilling, the perfluorocarbon tracer (PFT) perfluoromethyldecalin (PFMD; C₁₁F₂₀) will be continuously introduced to the drilling fluid (target concentration of ~1 ppm) to allow assessment of the extent to which the interior of drill cores have been exposed to contamination.

The second visit will take place after drilling operations in Hole U1309D and will focus on fluid sampling and borehole logging. Two Kuster Flow Through Sampler (FTS) (de Ronde et al., 2019) tools will be assembled in series and lowered to collect 600 mL borehole samples each in conjunction with the Elevated Temperature Borehole Sensor (ETBS). The Kuster FTS tools are mechanically triggered with a clock and will be set to trigger at depths based on intervals of interest from the recovered core material.

Finally, routine wireline logging will be performed using a triple combo logging tool string (caliper, density, resistivity, and natural gamma radiation), followed by the Formation MicroScanner (FMS)-sonic tool string. FMS data will be of particular interest because they present images of structural features and document fracture orientations. The sonic tool will measure wall rock seismic velocity. Prior to the deployment of the FMS, the hole will be filled with freshwater to enhance the quality of wall imagery (Expedition 304/305 Scientists, 2006). If time and circumstances permit (i.e., no marine mammals are in the area), the Versatile Seismic Imager (VSI) will be run to generate extended crustal architecture logs for syncing with new lithologic analysis.

5.2. Site U1309

The first operational task in Hole U1309D will be the collection of pristine fluid samples and thermal profile data from the borehole using the Kuster FTS tool and the sea trial of the Multi-Temperature Fluid Sampler tool (MTFS; Wheat et al., 2020), followed by remediation of the hole and hole deepening via RCB coring:

1. Deploy both Kuster FTS tools assembled with the ETBS to collect fluid samples from ~350 mbsf (~35°C) and ~600 mbsf (~60°C).
2. Deploy the MTFS (Figure F12) with the ETBS to total borehole depth to collect a range of samples. In the event that the first deployment is not completed successfully (i.e., if the majority of the samplers do not trigger), we have budgeted time for two MTFS deployments to allow a second attempt. However, if the first deployment appears successful (i.e., the majority of samplers have triggered), the second deployment would be canceled. It is worth noting a second deployment would be of lower quality because the borehole would already be disturbed from the first sampling.



Figure F12. MTFS assembled and ready for deployment on catwalk during IODP Expedition 385T (Wheat et al., 2020).

3. Deploy the Kuster FTS tools again to collect samples from deeper/hotter depth (~1200 mbsf or ~120°C) as well as a background sample from ~20 to 30 mbsf for comparison with the MTFS samples and for calibrating microbiological and organic analyses on deeper samples.
4. Deploy the reverse circulation junk basket (RCJB) fishing tool to remove a logging caliper presumed to have fallen to the bottom of the hole during Expedition 340T. Other fishing tools may be deployed if deemed appropriate such as a magnet or milling tool.
5. Deepen Hole U1309D with RCB coring to ~2060 mbsf.
6. Log (with flaked tools to protect electronics from high temperatures) from 1300 mbsf to as deep as temperatures allow.
7. Drill a new 80 m deep RCB hole in the vicinity of Hole U1309D (proposed Site AMDH-01A) aimed primarily at sampling porous zones in gabbro and diabase for microbiology and pore water chemistry.

We will implement a fluid sampling program in Hole U1309D, prior to hole disturbance, with the aim of collecting multiple pristine borehole fluid samples to examine microbiology and geochemistry across the known thermal limits for life. We will target fluid sampling at temperatures associated with mesophilic (~35°C) and thermophilic (~65° and 75°C) temperature ranges (and less than ~750 mbsf), with the ~75°C sample coming from an area in the borehole with presumed inflow of fluid. For lower temperature sampling, the Kuster FTS tool will be deployed, collecting ~600 mL of fluid from a target depth horizon, where the temperature is estimated based on prior thermal measurements in the hole. Higher temperature borehole fluids will be collected with the newly developed MTFS (Figure F12), which allows the simultaneous collection of up to twelve 1 L samples (Wheat et al., 2020). It operates with a shape memory alloy that triggers sampling at temperatures from 80° to 181°C (Wheat et al., 2020).

Following fluid sampling and hole remediation, we will core to a target depth of 2060 mbsf (9–10 bit runs), where the ambient temperature is predicted to be ~220°C based on the temperature gradient recorded during Expedition 340T (Blackman et al., 2014). Only gradual changes in lithology are expected from geophysical interpretations (Figure F2B). During Expedition 305, the hole was deepened by 1014 m in 40 days on site. We have assumed slower drilling rates in hotter conditions, down to 1 m/h below 2000 mbsf, and taken half-length RCB cores to account for challenging penetration conditions (Table T1). Core barrels will be run without core liners (plastic liners begin to melt at 80°C, and aluminum split cores are only marginally useful), with the contents shaken out into split core liners upon recovery, as done during IODP Expedition 376 (Brothers Arc; de Ronde et al., 2019). A Niskin bottle will be mounted on the camera frame during every lowering to collect water column samples directly above the reentry cone.

As with coring at proposed Site AMDH-02A, a PFT will be continuously introduced to the drilling fluid to allow assessment of the extent to which the interior of drill cores have been exposed to contamination.

The final operation in Hole U1309D will be logging. Depression of borehole temperatures during drilling and hole conditioning should allow a high proportion of the deepened hole to be logged. A standard triple combo logging tool string would chart hole conditions (caliper) and logs of density (Hostile Environment Litho-Density Sonde [HLDS]) and resistivity (High-Resolution Laterolog Array [HRLA]) will be most valuable for wall rock characterization. The FMS-sonic tool string would be run next to image structural features, document fracture orientations, and measure wall rock seismic velocity. If time and circumstances allow (i.e., no marine mammals in the area), we would also run the VSI. This will generate extended crustal architecture logs for syncing with new lithologic analysis of deep, hot gabbros (Objective 1).

An ~80 m deep RCB hole will be drilled at proposed Site AMDH-01A (Site U1309) with the aim of sampling for the third time the fault zone in gabbro and diabase sampled in Holes U1309B and U1309D. The hole will be located to allow triangulation of diabase contacts with the previous holes, with the aim of calculating orientations. The main aim of this hole is to collect zones of reaction porosity for microbiology and pore water sampling.

5.3. Alternate drilling locations

Proposed Site AMDH-03A is an alternate for proposed Site AMDH-02A and is located on a shelf midway between Expedition 357 Sites M0070 and M0071 (Figure F4). At Site M0071, largely serpentinites were recovered, with intercalations of chloritized gabbro and minor diabase. Site M0070 recovered a few meters of basaltic breccia, probably from a nearby volcanic cone erupted on the detachment surface. We anticipate a similar sequence through fault rocks and serpentinitized and talc-chlorite-tremolite altered ultramafic rocks as at proposed Site AMDH-02A. We would drill a pilot hole and then install a reentry system.

Proposed Site AMDH-05A is a contingency site that may include multiple single-bit holes drilled anywhere in an approved polygon (Figure F4). This alternate site would be used if operations at proposed Sites AMDH-01A, AMDH-02A, and AMDH-03A all fail.

6. Sampling and data sharing strategy

Shipboard and potential shore-based researchers should refer to the IODP Sample, Data, and Obligations Policy and Implementation Guidelines posted on the Web at <http://www.iodp.org/top-resources/program-documents/policies-and-guidelines>. This document outlines the policy for distributing IODP samples and data to research scientists, curators, and educators. The document also defines the obligations that sample and data recipients incur. The Sample Allocation Committee (SAC; composed of the two Co-Chief Scientists, Expedition Project Manager, and IODP Curator on shore and curatorial representative on board) will work with the entire scientific party to formulate a formal expedition-specific sampling plan for shipboard sampling. An orchestrated shore-based sampling effort is not planned.

Shipboard scientists will be expected to submit research plans and associated sample requests 6–8 months before the beginning of the expedition. Based on the submitted sample requests, the SAC will prepare a tentative sampling plan, which will be revised on the ship based on recovered materials and acquired data as well as collaborations that may evolve between scientists. Shore-based requests may be considered at that time if they are not in conflict with research plans by shipboard scientists. The SAC will make final decisions regarding each request in consultation with experts in the shipboard party.

All sample frequencies and sizes must be justified on a scientific basis and will depend on core recovery, the full spectrum of other requests, and the overall project objectives. The total number of samples for a requester must be in the range of what can be analyzed and published in ~2 y. Additional samples can be requested thereafter. Some redundancy of measurements is unavoidable, but minimizing the duplication of measurements among the shipboard party and approved shore-based collaborators will be an important factor in evaluating sample requests.

Recovery of critical intervals may result in considerable demand for samples from a limited amount of cored material. These intervals may require special handling, a higher sampling density, reduced sample size, or other strategies. A sampling strategy coordinated by the SAC will be required before critical intervals are sampled. In addition, the permanent archive, which is preserved and excluded from sampling for at least 5 y, will be the standard archive half of each core.

7. Risks and contingency

The condition of Hole U1309D is unknown. The operations plan assumes that the caliper can be reached and removed by fishing or milling. If hole conditions are problematic, the priority will be an attempt to remediate the hole and to determine if future work in Hole U1309D is practical.

Significant risks are associated with the first sea trials of the recently developed MTFS, including failure of the intended functions or loss of the tool. Some issues may be addressed and fixed in real time, whereas others may result in termination of the test activity.

Multiple attempts may be needed to start the pilot hole in bare rock at proposed Site AMDH-02A, but it has been done successfully before. Setting a reentry system has a small risk, and issues can typically be addressed in real time.

Weather can always play a role. At this time, Expedition 399 is scheduled to occur during a favorable weather window, and the operations plan has adequate contingency time, minimizing this risk.

8. Expedition scientists and scientific participants

The current list of participants for Expedition 399 can be found at http://iodp.tamu.edu/science-ops/expeditions/atlantis_massif_blocks_of_life.html.

References

- Allen, D.E., and Seyfried, W.E., 2003. Compositional controls on vent fluids from ultramafic-hosted hydrothermal systems at mid-ocean ridges: an experimental study at 400°C, 500 bars. *Geochimica et Cosmochimica Acta*, 67(8):1531–1542. [https://doi.org/10.1016/S0016-7037\(02\)01173-0](https://doi.org/10.1016/S0016-7037(02)01173-0)
- Allen, D.E., and Seyfried, W.E., 2004. Serpentinization and heat generation: constraints from Lost City and Rainbow hydrothermal systems. *Geochimica et Cosmochimica Acta*, 68(6):1347–1354. <https://doi.org/10.1016/j.gca.2003.09.003>
- Allen, D.E., and Seyfried, W.E., 2005. REE controls in ultramafic hosted MOR hydrothermal systems: an experimental study at elevated temperature and pressure. *Geochimica et Cosmochimica Acta*, 69(3):675–683. <https://doi.org/10.1016/j.gca.2004.07.016>
- Andreani, M., and Ménez, B., 2019. New perspectives on abiotic organic synthesis and processing during hydrothermal alteration of the oceanic lithosphere. In Orcutt, B.N., Daniel, I., and Dasgupta, R. (Eds.), *Deep Carbon: Past to Present*. Cambridge, England (Cambridge University Press), 447–479. <https://doi.org/10.1017/9781108677950>
- Andreani, M., Muñoz, M., Marcaillou, C., and Delacour, A., 2013. μ XANES study of iron redox state in serpentine during oceanic serpentinization. *Lithos*, 178:70–83. <https://doi.org/10.1016/j.lithos.2013.04.008>
- Bach, W., Garrido, C.J., Paulick, H., Harvey, J., and Rosner, M., 2004. Seawater-peridotite interactions: first insights from ODP Leg 209, MAR 15°N. *Geochemistry, Geophysics, Geosystems*, 5(9):Q09F26. <https://doi.org/10.1029/2004GC000744>
- Bach, W., and Humphris, S.E., 1999. Relationship between the Sr and O isotope compositions of hydrothermal fluids and the spreading and magma-supply rates at oceanic spreading centers. *Geology*, 27(12):1067–1070. [https://doi.org/10.1130/0091-7613\(1999\)027<1067:RBTSAO>2.3.CO;2](https://doi.org/10.1130/0091-7613(1999)027<1067:RBTSAO>2.3.CO;2)
- Beard, J.S., Frost, B.R., Fryer, P., McCaig, A., Searle, R., Ildefonse, B., Zinin, P., and Sharma, S.K., 2009. Onset and progression of serpentinization and magnetite formation in olivine-rich troctolite from IODP Hole U1309D. *Journal of Petrology*, 50(3):387–403. <https://doi.org/10.1093/petrology/egp004>
- Blackman, D., Slagle, A., Harding, A., Guerin, G., and McCaig, A., 2013. IODP Expedition 340T: borehole logging at Atlantis Massif oceanic core complex. *Scientific Drilling*, 15:31–35. <https://doi.org/10.2204/iodp.sd.15.04.2013>
- Blackman, D.K., Cann, J.R., Janssen, B., and Smith, D.K., 1998. Origin of extensional core complexes: evidence from the Mid-Atlantic Ridge at Atlantis Fracture Zone. *Journal of Geophysical Research: Solid Earth*, 103(B9):21315–21333. <https://doi.org/10.1029/98JB01756>
- Blackman, D.K., Ildefonse, B., John, B.E., Ohara, Y., Miller, D.J., Abe, N., Abratis, M., Andal, E.S., Andreani, M., Awaji, S., Beard, J.S., Brunelli, D., Charney, A.B., Christie, D.M., Collins, J., Delacour, A.G., Delius, H., Drouin, M., Einaudi, F., Escartin, J., Frost, B.R., Früh-Green, G., Fryer, P.B., Gee, J.S., Godard, M., Grimes, C.B., Halfpenny, A., Hansen, H.E., Harris, A.C., Tamura, A., Hayman, N.W., Hellebrand, E., Hirose, T., Hirth, J.G., Ishimaru, S., Johnson, K.T.M., Karner, G.D., Linek, M., MacLeod, C.J., Maeda, J., Mason, O.U., McCaig, A.M., Michibayashi, K., Morris, A., Nakagawa, T., Nozaka, T., Rosner, M., Searle, R.C., Suhr, G., Tominaga, M., von der Handt, A., Yamasaki, T., and Zhao, X., 2011. Drilling constraints on lithospheric accretion and evolution at Atlantis Massif, Mid-Atlantic Ridge 30°N. *Journal of Geophysical Research: Solid Earth*, 116(B7):B07103. <https://doi.org/10.1029/2010JB007931>
- Blackman, D.K., Karson, J.A., Kelley, D.S., Cann, J.R., Früh-Green, G.L., Gee, J.S., Hurst, S.D., John, B.E., Morgan, J., Nooner, S.L., Ross, D.K., Schroeder, T.J., and Williams, E.A., 2002. Geology of the Atlantis Massif (Mid-Atlantic Ridge, 30°N): implications for the evolution of an ultramafic oceanic core complex. *Marine Geophysical Research*, 23(5):443–469. <https://doi.org/10.1023/B:MARI.0000018232.14085.75>
- Blackman, D.K., Slagle, A.L., Guerin, G., and Harding, A., 2014. Geophysical signatures of past and present hydration within a young oceanic core complex. *Geophysical Research Letters*, 41(4):1179–1186. <https://doi.org/10.1002/2013GL058111>
- Boschi, C., Früh-Green, G.L., Delacour, A., Karson, J.A., and Kelley, D.S., 2006. Mass transfer and fluid flow during detachment faulting and development of an oceanic core complex, Atlantis Massif (MAR 30°N). *Geochemistry, Geophysics, Geosystems*, 7(1):Q01004. <https://doi.org/10.1029/2005GC001074>

- Bourdelle, F., and Cathelineau, M., 2015. Low-temperature chlorite geothermometry: a graphical representation based on a T–R₂₊–Si diagram. *European Journal of Mineralogy*, 27(5):617–626. <https://doi.org/10.1127/ejm/2015/0027-2467>
- Bradley, A.S., Hayes, J.M., and Summons, R.E., 2009. Extraordinary ¹³C enrichment of diether lipids at the Lost City hydrothermal field indicates a carbon-limited ecosystem. *Geochimica et Cosmochimica Acta*, 73(1):102–118. <https://doi.org/10.1016/j.gca.2008.10.005>
- Brazelton, W.J., and Baross, J.A., 2010. Metagenomic comparison of two *Thiomicrospira* lineages inhabiting contrasting deep-sea hydrothermal environments. *PLoS One*, 5(10):e13530. <https://doi.org/10.1371/journal.pone.0013530>
- Brazelton, W.J., Thornton, C.N., Hyer, A., Twing, K.L., Longino, A.A., Lang, S.Q., Lilley, M.D., Früh-Green, G.L., and Schrenk M.O., 2017. Metagenomic identification of active methanogens and methanotrophs in serpentinite springs of the Voltri Massif, Italy. *PeerJ*, 5:e2945. <https://doi.org/10.7717/peerj.2945>
- Brazelton, W.J., Ludwig, K.A., Sogin, M.L., Andreishcheva, E.N., Kelley, D.S., Shen, C.-C., Edwards, R.L., and Baross, J.A., 2010. Archaea and bacteria with surprising microdiversity show shifts in dominance over 1,000-year time scales in hydrothermal chimneys. *Proceedings of the National Academy of Sciences of the United States of America*, 107(4):1612–1617. <https://doi.org/10.1073/pnas.0905369107>
- Brazelton, W.J., Schrenk, M.O., Kelley, D.S., and Baross, J.A., 2006. Methane- and sulfur-metabolizing microbial communities dominate the Lost City hydrothermal field ecosystem. *Applied and Environmental Microbiology*, 72(9):6257–6270. <https://doi.org/10.1128/AEM.00574-06>
- Canales, J.P., Tucholke, B.E., and Collins, J.A., 2004. Seismic reflection imaging of an oceanic detachment fault: Atlantis megamullion (Mid-Atlantic Ridge, 30°10'N). *Earth and Planetary Science Letters*, 222(2):543–560. <https://doi.org/10.1016/j.epsl.2004.02.023>
- Canales, J.P., Tucholke, B.E., Xu, M., Collins, J.A., and DuBois, D.L., 2008. Seismic evidence for large-scale compositional heterogeneity of oceanic core complexes. *Geochemistry, Geophysics, Geosystems*, 9(8):Q08002. <https://doi.org/10.1029/2008GC002009>
- Cann, J.R., Blackman, D.K., Smith, D.K., McAllister, E., Janssen, B., Mello, S., Avgerinos, E., Pascoe, A.R., and Escartin, J., 1997. Corrugated slip surfaces formed at ridge–transform intersections on the Mid-Atlantic Ridge. *Nature*, 385(6614):329–332. <https://doi.org/10.1038/385329a0>
- Cann, J.R., McCaig, A.M., and Yardley, B.W.D., 2015. Rapid generation of reaction permeability in the roots of black smoker systems, Troodos ophiolite, Cyprus. *Geofluids*, 15(1–2):179–192. <https://doi.org/10.1111/gfl.12117>
- de Ronde, C.E.J., Humphris, S.E., Höfig, T.W., Brandl, P.A., Cai, L., Cai, Y., Caratori Tontini, F., Deans, J.R., Farough, A., Jamieson, J.W., Kolandaivelu, K.P., Kutovaya, A., Labonté, J.M., Martin, A.J., Massiot, C., McDermott, J.M., McIntosh, I.M., Nozaki, T., Pellizari, V.H., Reyes, A.G., Roberts, S., Rouxel, O., Schlicht, L.E.M., Seo, J.H., Straub, S.M., Strehlow, K., Takai, K., Tanner, D., Tepley III, F.J., and Zhang, C., 2019. Expedition 376 methods. In de Ronde, C.E.J., Humphris, S.E., Höfig, T.W., and the Expedition 376 Scientists, Brothers Arc Flux. *Proceedings of the International Ocean Discovery Program*, 376: College Station, TX (International Ocean Discovery Program). <https://doi.org/10.14379/iodp.proc.376.102.2019>
- Denny, A.R., Kelley, D.S., and Früh-Green, G.L., 2016. Geologic evolution of the Lost City Hydrothermal Field. *Geochemistry, Geophysics, Geosystems*, 17(2):375–394. <https://doi.org/10.1002/2015GC005869>
- Detrick, R.S., and Collins, J.A., 1998. Seismic structure of ultramafics exposed at shallow crustal levels in the Mid-Atlantic Ridge rift valley at 15°N. *Eos, Transactions of the American Geophysical Union*, 79:F800.
- Dick, H.J.B., MacLeod, C.J., Blum, P., Abe, N., Blackman, D.K., Bowles, J.A., Cheadle, M.J., Cho, K., Ciazela, J., Deans, J.R., Edgcomb, V.P., Ferrando, C., France, L., Ghosh, B., Ildefonse, B.M., Kendrick, M.A., Koepke, J.H., Leong, J.A.M., Chuangzhou, L., Qiang, M., Morishita, T., Morris, A., Natland, J.H., Nozaka, T., Pluempner, O., Sanfilippo, A., Sylvan, J.B., Tivey, M.A., Tribuzio, R., and Viegas, L.G.F., 2017. Expedition 360 summary. In MacLeod, C.J., Dick, H.J.B., Blum, P., and the Expedition 360 Scientists, Southwest Indian Ridge Lower Crust and Moho. *Proceedings of the International Ocean Discovery Program*, 360: College Station, TX (International Ocean Discovery Program). <https://doi.org/10.14379/iodp.proc.360.101.2017>
- Drouin, M., Godard, M., Ildefonse, B., Bruguier, O., and Garrido, C.J., 2009. Geochemical and petrographic evidence for magmatic impregnation in the oceanic lithosphere at Atlantis Massif, Mid-Atlantic Ridge (IODP Hole U1309D, 30°N). *Chemical Geology*, 264(1):71–88. <https://doi.org/10.1016/j.chemgeo.2009.02.013>
- Escartín, J., and Canales, J.P., 2011. Detachments in oceanic lithosphere: deformation, magmatism, fluid flow, and ecosystems. *Eos, Transactions American Geophysical Union*, 92(4):31. <https://doi.org/10.1029/2011EO040003>
- Escartín, J., John, B., Cannat, M., Olive, J.-A., Cheadle, M., Früh-Green, G., and Cotterill, C., 2022. Tectonic termination of oceanic detachment faults, with constraints on tectonic uplift and mass wasting related erosion rates. *Earth and Planetary Science Letters*, 584:117449. <https://doi.org/10.1016/j.epsl.2022.117449>
- Expedition 304/305 Scientists, 2006. Expedition 304/305 summary. In Blackman, D.K., Ildefonse, B., John, B.E., Ohara, Y., Miller, D.J., MacLeod, C.J., and the Expedition 304/305 Scientist, *Proceedings of the Integrated Ocean Drilling Program*, 304/305: College Station, TX (Integrated Ocean Drilling Program Management International, Inc.). <https://doi.org/10.2204/iodp.proc.304305.101.2006>
- Ferrando, C., Godard, M., Ildefonse, B., and Rampone, E., 2018. Melt transport and mantle assimilation at Atlantis Massif (IODP Site U1309): constraints from geochemical modeling. *Lithos*, 323:24–43. <https://doi.org/10.1016/j.lithos.2018.01.012>
- Foustoukos, D.I., Savov, I.P., and Janecky, D.R., 2008. Chemical and isotopic constraints on water/rock interactions at the Lost City hydrothermal field, 30°N Mid-Atlantic Ridge. *Geochimica et Cosmochimica Acta*, 72(22):5457–5474. <https://doi.org/10.1016/j.gca.2008.07.035>
- Foustoukos, D.I., and Seyfried, W.E., 2004. Hydrocarbons in hydrothermal vent fluids: the role of chromium-bearing catalysts. *Science*, 304(5673):1002–1005. <https://doi.org/10.1126/science.1096033>

- Frost, B.R., 1985. On the stability of sulfides, oxides, and native metals in serpentinite. *Journal of Petrology*, 26(1):31–63. <https://doi.org/10.1093/petrology/26.1.31>
- Frost, B.R., Beard, J.S., McCaig, A., and Condliffe, E., 2008. The formation of micro-rodingites from IODP Hole U1309D: key to understanding the process of serpentinization. *Journal of Petrology*, 49(9):1579–1588. <https://doi.org/10.1093/petrology/egn038>
- Früh-Green, G.L., Connolly, J.A.D., Plas, A., Kelley, D.S., and Grobéty, B., 2004. Serpentinization of oceanic peridotites: implications for geochemical cycles and biological activity. In Wilcock, W.S.D., Delong, E.F., Kelley, D.S., Baross, J.A., and Cary, S.C. (Eds.), *The Subseafloor Biosphere at Mid-Ocean Ridges*. Geophysical Monograph, 144: 119–136. <https://doi.org/10.1029/144GM08>
- Früh-Green, G.L., Orcutt, B.N., and Green, S., 2015. Expedition 357 Scientific Prospectus: Atlantis Massif Serpentinization and Life. International Ocean Discovery Program. <https://doi.org/10.14379/iodp.sp.357.2015>
- Früh-Green, G.L., Orcutt, B.N., Green, S., Cotterill, C., and the Expedition 357 Scientists, 2016. Expedition 357 Preliminary Report: Atlantis Massif Serpentinization and Life. International Ocean Discovery Program. <https://doi.org/10.14379/iodp.pr.357.2016>
- Früh-Green, G.L., Orcutt, B.N., Green, S.L., Cotterill, C., Morgan, S., Akizawa, N., Bayrakci, G., Behrmann, J.-H., Boschi, C., Brazelton, W.J., Cannat, M., Dunkel, K.G., Escartin, J., Harris, M., Herrero-Bervera, E., Hesse, K., John, B.E., Lang, S.Q., Lilley, M.D., Liu, H.-Q., Mayhew, L.E., McCaig, A.M., Menez, B., Morono, Y., Quéméneur, M., Rouméjon, S., Sandaruwan Ratnayake, A., Schrenk, M.O., Schwarzenbach, E.M., Twing, K.I., Weis, D., Whattam, S.A., Williams, M., and Zhao, R., 2017. Expedition 357 summary. In Früh-Green, G.L., Orcutt, B.N., Green, S.L., Cotterill, C., and the Expedition 357 Scientists, *Atlantis Massif Serpentinization and Life*. Proceedings of the International Ocean Discovery Program, 357: College Station, TX (International Ocean Discovery Program). <https://doi.org/10.14379/iodp.proc.357.101.2017>
- Früh-Green, G.L., Orcutt, B.N., Rouméjon, S., Lilley, M.D., Morono, Y., Cotterill, C., Green, S., Escartin, J., John, B.E., McCaig, A.M., Cannat, M., Menez, B., Schwarzenbach, E.M., Williams, M.J., Morgan, S., Lang, S.Q., Schrenk, M.O., Brazelton, W.J., Akizawa, N., Boschi, C., Dunkel, K.G., Quéméneur, M., Whattam, S.A., Mayhew, L., Harris, M., Bayrakci, G., Behrmann, J.-H., Herrero-Bervera, E., Hesse, K., Liu, H.-Q., Ratnayake, A.S., Twing, K., Weis, D., Zhao, R., and Bilinker, L., 2018. Magmatism, serpentinization and life: insights through drilling the Atlantis Massif (IODP Expedition 357). *Lithos*, 323:137–155. <https://doi.org/10.1016/j.lithos.2018.09.012>
- Godard, M., Awaji, S., Hansen, H., Hellebrand, E., Brunelli, D., Johnson, K., Yamasaki, T., Maeda, J., Abratis, M., Christie, D., Kato, Y., Mariet, C., and Rosner, M., 2009. Geochemistry of a long in-situ section of intrusive slow-spread oceanic lithosphere: results from IODP Site U1309 (Atlantis Massif, 30°N Mid-Atlantic-Ridge). *Earth and Planetary Science Letters*, 279(1–2):110–122. <https://doi.org/10.1016/j.epsl.2008.12.034>
- Goordial, J., D'Angelo, T., Labonté, J.M., Poulton, N.J., Brown, J.M., Stepanauskas, R., Früh-Green, G.L., Orcutt, B.N., and Dubilier, N., 2021. Microbial diversity and function in shallow subsurface sediment and oceanic lithosphere of the Atlantis Massif. *MBio*, 12(4):e00490–00421. <https://journals.asm.org/doi/abs/10.1128/mBio.00490-21>
- Grimes, C.B., John, B.E., Cheadle, M.J., and Wooden, J.L., 2008. Protracted construction of gabbroic crust at a slow spreading ridge; constraints from ²⁰⁶Pb/²³⁸U zircon ages from Atlantis Massif and IODP Hole U1309D (30°N, MAR). *Geochemistry, Geophysics, Geosystems*, 9(8):Q08012. <https://doi.org/10.1029/2008GC002063>
- Harding, A.J., Arnulf, A.F., and Blackman, D.K., 2016. Velocity structure near IODP Hole U1309D, Atlantis Massif, from waveform inversion of streamer data and borehole measurements. *Geochemistry, Geophysics, Geosystems*, 17(6):1990–2014. <https://doi.org/10.1002/2016GC006312>
- Henig, A.S., Blackman, D.K., Harding, A.J., Canales, J.-P., and Kent, G.M., 2012. Downward continued multichannel seismic refraction analysis of Atlantis Massif oceanic core complex, 30°N, Mid-Atlantic Ridge. *Geochemistry, Geophysics, Geosystems*, 13(5):Q0AG07. <https://doi.org/10.1029/2012GC004059>
- Heuer, V.B., Inagaki, F., Morono, Y., Kubo, Y., Spivack, A.J., Viehweger, B., Treude, T., Beulig, F., Schubotz, F., Tonai, S., Bowden, S.A., Cramm, M., Henkel, S., Hirose, T., Homola, K., Hoshino, T., Ijiri, A., Imachi, H., Kamiya, N., Kaneko, M., Lagostina, L., Manners, H., McClelland, H.-L., Metcalfe, K., Okutsu, N., Pan, D., Raudsepp, M.J., Sauvage, J., Tsang, M.-Y., Wang, D.T., Whitaker, E., Yamamoto, Y., Yang, K., Maeda, L., Adhikari, R.R., Glombitza, C., Hamada, Y., Kallmeyer, J., Wendt, J., Wörmer, L., Yamada, Y., Kinoshita, M., and Hinrichs, K.-U., 2020. Temperature limits to deep seafloor life in the Nankai Trough subduction zone. *Science*, 370(6521):1230–1234. <https://doi.org/10.1126/science.abd7934>
- Ildefonse, B., Blackman, D., John, B.E., Ohara, Y., Miller, D.J., MacLeod, C., and the Integrated Ocean Drilling Program Expeditions 304/305 Science Party, 2007. Oceanic core complexes and crustal accretion at slow-spreading ridges. *Geology*, 35(7):623–626. <https://doi.org/10.1130/G23531A.1>
- Jørgensen, S.L., and Zhao, R., 2016. Microbial inventory of deeply buried oceanic crust from a young ridge flank. *Frontiers in Microbiology*, 7:820. <https://doi.org/10.3389/fmicb.2016.00820>
- Kallmeyer, J., 2017. Contamination control for scientific drilling operations. In Sariaslani, S. and Gadd, G.M., *Advances in Applied Microbiology* (Volume 98). Cambridge, MA (Academic Press), 61–91. <https://doi.org/10.1016/bs.aambs.2016.09.003>
- Karson, J.A., Früh-Green, G.L., Kelley, D.S., Williams, E.A., Yoerger, D.R., and Jakuba, M., 2006. Detachment shear zone of the Atlantis Massif core complex, Mid-Atlantic Ridge, 30°N. *Geochemistry, Geophysics, Geosystems*, 7(6):Q06016. <https://doi.org/10.1029/2005GC001109>
- Kelemen, P.B., Matter, J., Streit, E.E., Rudge, J.F., Curry, W.B., and Blusztajn, J., 2011. Rates and mechanisms of mineral carbonation in peridotite: natural processes and recipes for enhanced, in situ CO₂ capture and storage. *Annual Review of Earth and Planetary Sciences*, 39(1):545–576. <https://doi.org/10.1146/annurev-earth-092010-152509>
- Kelley, D.S., Baross, J.A., and Delaney, J.R., 2002. Volcanoes, fluids, and life at mid-ocean ridge spreading centers. *Annual Review of Earth and Planetary Sciences*, 30(1):385–491. <https://doi.org/10.1146/annurev.earth.30.091201.141331>

- Kelley, D.S., and Früh-Green, G.L., 1999. Abiogenic methane in deep-seated mid-ocean ridge environments: Insights from stable isotope analyses. *Journal of Geophysical Research: Solid Earth*, 104(B5):10439–10460. <https://doi.org/10.1029/1999JB900058>
- Kelley, D.S., and Früh-Green, G.L., 2001. Volatile lines of descent in submarine plutonic environments: insights from stable isotope and fluid inclusion analyses. *Geochimica et Cosmochimica Acta*, 65(19):3325–3346. [https://doi.org/10.1016/S0016-7037\(01\)00667-6](https://doi.org/10.1016/S0016-7037(01)00667-6)
- Kelley, D.S., Karson, J.A., Blackman, D.K., Früh-Green, G.L., Butterfield, D.A., Lilley, M.D., Olson, E.J., Schrenk, M.O., Roe, K.K., Lebon, G.T., Rivizzigno, P., and the AT3-60 Shipboard Party, 2001. An off-axis hydrothermal vent field near the Mid-Atlantic Ridge at 30°N. *Nature*, 412(6843):145–149. <https://doi.org/10.1038/35084000>
- Kelley, D.S., Karson, J.A., Früh-Green, G., and Schrenk, M.O., 2002. Ultramafic-hosted hydrothermal systems: the Lost City Field as a possible guide for early life. *Astrobiology*, 2(4):449–450.
- Kelley, D.S., Karson, J.A., Früh-Green, G.L., Yoerger, D.R., Shank, T.M., Butterfield, D.A., Hayes, J.M., Schrenk, M.O., Olson, E.J., Proskurowski, G., Jakuba, M., Bradley, A., Larson, B., Ludwig, K., Glickson, D., Buckman, K., Bradley, A.S., Brazelton, W.J., Roe, K., Elend, M.J., Delacour, A.I., Bernasconi, S.M., Lilley, M.D., Baross, J.A., Summons, R.E., and Sylva, S.P., 2005. A serpentinite-hosted ecosystem: the Lost City hydrothermal field. *Science*, 307(5714):1428–1434. <https://doi.org/10.1126/science.1102556>
- Klein, F., Bach, W., and McCollom, T.M., 2013. Compositional controls on hydrogen generation during serpentinization of ultramafic rocks. *Lithos*, 178:55–69. <https://doi.org/10.1016/j.lithos.2013.03.008>
- Klein, F., Grozeva, N.G., and Seewald, J.S., 2019. Abiotic methane synthesis and serpentinization in olivine-hosted fluid inclusions. *Proceedings of the National Academy of Sciences of the United States of America*, 116(36):17666–17672. <https://doi.org/10.1073/pnas.1907871116>
- Lang, S.Q., and Brazelton, W.J., 2020. Habitability of the marine serpentinite subsurface: a case study of the Lost City hydrothermal field. *Philosophical Transactions of the Royal Society A: Mathematical, Physical and Engineering Sciences*, 378(2165):20180429. <https://doi.org/10.1098/rsta.2018.0429>
- Lang, S.Q., Butterfield, D.A., Schulte, M., Kelley, D.S., and Lilley, M.D., 2010. Elevated concentrations of formate, acetate and dissolved organic carbon found at the Lost City hydrothermal field. *Geochimica et Cosmochimica Acta*, 74(3):941–952. <https://doi.org/10.1016/j.gca.2009.10.045>
- Lang, S.Q., Früh-Green, G.L., Bernasconi, S.M., Brazelton, W.J., Schrenk, M.O., and McGonigle, J.M., 2018. Deeply-sourced formate fuels sulfate reducers but not methanogens at Lost City hydrothermal field. *Scientific Reports*, 8(1):755. <https://doi.org/10.1038/s41598-017-19002-5>
- Lang, S.Q., Lilley, M.D., Baumberger, T., Früh-Green, G.L., Walker, S.L., Brazelton, W.J., Kelley, D.S., Elend, M., Butterfield, D.A., and Mau, A.J., 2021. Extensive decentralized hydrogen export from the Atlantis Massif. *Geology*, 49(7):851–856. <https://doi.org/10.1130/G48322.1>
- Liebmann, J., Schwarzenbach, E.M., Früh-Green, G.L., Boschi, C., Rouméjon, S., Strauss, H., Wiechert, U., and John, T., 2018. Tracking water-rock interaction at the Atlantis Massif (MAR, 30°N) using sulfur geochemistry. *Geochemistry, Geophysics, Geosystems*, 19(11):4561–4583. <https://doi.org/10.1029/2018GC007813>
- Lissenberg, C.J., and MacLeod, C.J., 2017. A reactive porous flow control on mid-ocean ridge magmatic evolution. *Journal of Petrology*, 57(11-12):2195–2220. <https://doi.org/10.1093/petrology/egw074>
- Lowell, R.P., 2017. A fault-driven circulation model for the Lost City hydrothermal field. *Geophysical Research Letters*, 44(6):2703–2709. <https://doi.org/10.1002/2016GL072326>
- Ludwig, K.A., Shen, C.-C., Kelley, D.S., Cheng, H., and Edwards, R.L., 2011. U–Th systematics and ²³⁰Th ages of carbonate chimneys at the Lost City hydrothermal field. *Geochimica et Cosmochimica Acta*, 75(7):1869–1888. <https://doi.org/10.1016/j.gca.2011.01.008>
- Martin, W., Baross, J., Kelley, D., and Russell, M.J., 2008. Hydrothermal vents and the origin of life. *Nature Reviews Microbiology*, 6(11):805–814. <https://doi.org/10.1038/nrmicro1991>
- Mason, O.U., Nakagawa, T., Rosner, M., Van Nostrand, J.D., Zhou, J., Maruyama, A., Fisk, M.R., and Giovannoni, S.J., 2010. First investigation of the microbiology of the deepest layer of ocean crust. *PLoS One*, 5(11):e15399. <https://doi.org/10.1371/journal.pone.0015399>
- McCaig, A.M., Delacour, A., Fallick, A.E., Castelain, T., and Früh-Green, G.L., 2010. Detachment fault control on hydrothermal circulation systems: interpreting the subsurface beneath the TAG hydrothermal field using the isotopic and geological evolution of oceanic core complexes in the Atlantic. In Rona, P., Devey, C.W., Dymont, J., and Murton, B.J. (Eds.), *Diversity of Hydrothermal Systems on Slow Spreading Ocean Ridges*. *Geophysical Monograph*, 188:207–239. <https://doi.org/10.1029/2008GM000729>
- McCaig, A.M., Früh-Green, G.L., Kelemen, P., and Teagle, D.A.H., 2020. Serpentinite in the Earth system. *Philosophical Transactions of the Royal Society A: Mathematical, Physical and Engineering Sciences*, 378(2165):20190332. <https://doi.org/10.1098/rsta.2019.0332>
- McCaig, A.M., and Harris, M., 2012. Hydrothermal circulation and the dike-gabbro transition in the detachment mode of slow seafloor spreading. *Geology*, 40(4):367–370. <https://doi.org/10.1130/G32789.1>
- McCollom, T.M., and Bach, W., 2009. Thermodynamic constraints on hydrogen generation during serpentinization of ultramafic rocks. *Geochimica et Cosmochimica Acta*, 73(3):856–875. <https://doi.org/10.1016/j.gca.2008.10.032>
- McCollom, T.M., Klein, F., Robbins, M., Moskowitz, B., Berquó, T.S., Jöns, N., Bach, W., and Templeton, A., 2016. Temperature trends for reaction rates, hydrogen generation, and partitioning of iron during experimental serpentinization of olivine. *Geochimica et Cosmochimica Acta*, 181:175–200. <https://doi.org/10.1016/j.gca.2016.03.002>
- McCollom, T.M., and Seewald, J.S., 2007. Abiotic synthesis of organic compounds in deep-sea hydrothermal environments. *Chemical Reviews*, 107(2):382–401. <https://doi.org/10.1021/cr0503660>
- McCollom, T.M., and Seewald, J.S., 2013. Serpentinization, hydrogen, and life. *Elements*, 9(2):129–134. <https://doi.org/10.2113/gselements.9.2.129>

- McDermott, J.M., Seewald, J.S., German, C.R., and Sylva, S.P., 2015. Pathways for abiotic organic synthesis at submarine hydrothermal fields. *Proceedings of the National Academy of Sciences of the United States of America*, 112(25):7668–7672. <https://doi.org/10.1073/pnas.1506295112>
- McGonigle, J.M., Lang, S.Q., Brazelton, W.J., and Parales, R.E., 2020. Genomic evidence for formate Metabolism by Chloroflexi as the key to unlocking deep carbon in Lost City microbial ecosystems. *Applied and Environmental Microbiology*, 86(8):e02583-02519. <https://doi.org/10.1128/AEM.02583-19>
- Méhay, S., Früh-Green, G.L., Lang, S.Q., Bernasconi, S.M., Brazelton, W.J., Schrenk, M.O., Schaeffer, P., and Adam, P., 2013. Record of archaeal activity at the serpentinite-hosted Lost City hydrothermal field. *Geobiology*, 11(6):570–592. <https://doi.org/10.1111/gbi.12062>
- Ménez, B., Pisapia, C., Andreani, M., Jamme, F., Vanbellingen, Q.P., Brunelle, A., Richard, L., Dumas, P., and Réfrégiers, M., 2018. Abiotic synthesis of amino acids in the recesses of the oceanic lithosphere. *Nature*, 564(7734):59–63. <https://doi.org/10.1038/s41586-018-0684-z>
- Morris, A., Gee, J.S., Pressling, N., John, B.E., MacLeod, C.J., Grimes, C.B., and Searle, R.C., 2009. Footwall rotation in an oceanic core complex quantified using reoriented Integrated Ocean Drilling Program core samples. *Earth and Planetary Science Letters*, 287(1–2):217–228. <https://doi.org/10.1016/j.epsl.2009.08.007>
- Motamedi, S., Orcutt, B.N., Früh-Green, G.L., Twing, K.I., Pendleton, H.L., and Brazelton, W.J., 2020. Microbial residents of the Atlantis Massif's shallow serpentinite subsurface. *Applied and Environmental Microbiology*, 86(11):e00356-00320. <https://doi.org/10.1128/AEM.00356-20>
- Nozaka, T., and Fryer, P., 2011. Alteration of the oceanic lower crust at a slow-spreading axis: insight from vein-related zoned halos in olivine gabbro from Atlantis Massif, Mid-Atlantic Ridge. *Journal of Petrology*, 52(4):643–664. <https://doi.org/10.1093/petrology/egq098>
- Nozaka, T., Fryer, P., and Andreani, M., 2008. Formation of clay minerals and exhumation of lower-crustal rocks at Atlantis Massif, Mid-Atlantic Ridge. *Geochemistry, Geophysics, Geosystems*, 9(11):Q11005. <https://doi.org/10.1029/2008GC002207>
- Olive, J.-A., Behn, M.D., and Tucholke, B.E., 2010. The structure of oceanic core complexes controlled by the depth distribution of magma emplacement. *Nature Geoscience*, 3(7):491–495. <https://doi.org/10.1038/ngeo888>
- Pendleton, H.L., Twing, K.I., Motamedi, S., and Brazelton, W.J., 2021. Potential microbial contamination from drilling lubricants into seafloor rock cores. *Scientific Drilling*, 29:49–57. <https://doi.org/10.5194/sd-29-49-2021>
- Pisapia, C., Jamme, F., Duponchel, L., and Ménez, B., 2018. Tracking hidden organic carbon in rocks using chemometrics and hyperspectral imaging. *Scientific Reports*, 8(1):2396. <https://doi.org/10.1038/s41598-018-20890-4>
- Proskurowski, G., Lilley, M.D., Seewald, J.S., Früh-Green, G.L., Olson, E.J., Lupton, J.E., Sylva, S.P., and Kelley, D.S., 2008. Abiogenic hydrocarbon production at Lost City hydrothermal field. *Science*, 319(5863):604–607. <https://doi.org/10.1126/science.1151194>
- Quéménéur, M., Erauso, G., Frouin, E., Zeghal, E., Vandecasteele, C., Ollivier, B., Tamburini, C., Garel, M., Ménez, B., and Postec, A., 2019. Hydrostatic pressure helps to cultivate an original anaerobic bacterium from the Atlantis Massif seafloor (IODP Expedition 357): *Petrocella atlantisensis* gen. nov. sp. nov. *Frontiers in Microbiology*, 10:1497. <https://doi.org/10.3389/fmicb.2019.01497>
- Rouméjon, S., Andreani, M., and Früh-Green, G.L., 2019. Antigorite crystallization during oceanic retrograde serpentinization of abyssal peridotites. *Contributions to Mineralogy and Petrology*, 174(7):60. <https://doi.org/10.1007/s00410-019-1595-1>
- Schoolmeesters, N., Cheadle, M.J., John, B.E., Reiners, P.W., Gee, J., and Grimes, C.B., 2012. The cooling history and the depth of detachment faulting at the Atlantis Massif oceanic core complex. *Geochemistry, Geophysics, Geosystems*, 13(10):Q0AG12. <https://doi.org/10.1029/2012GC004314>
- Schrenk, M.O., Brazelton, W.J., and Lang, S.Q., 2013. Serpentinization, carbon, and deep life. *Reviews in Mineralogy and Geochemistry*, 75(1):575–606. <https://doi.org/10.2138/rmg.2013.75.18>
- Schrenk, M.O., Kelley, D.S., Bolton, S.A., and Baross, J.A., 2004. Low archaeal diversity linked to seafloor geochemical processes at the Lost City hydrothermal field, Mid-Atlantic Ridge. *Environmental Microbiology*, 6(10):1086–1095. <https://doi.org/10.1111/j.1462-2920.2004.00650.x>
- Schroeder, T., and John, B.E., 2004. Strain localization on an oceanic detachment fault system, Atlantis Massif, 30°N, Mid-Atlantic Ridge. *Geochemistry, Geophysics, Geosystems*, 5(11):Q11007. <https://doi.org/10.1029/2004GC000728>
- Seyfried, W.E., Pester, N.J., Tutolo, B.M., and Ding, K., 2015. The Lost City hydrothermal system: constraints imposed by vent fluid chemistry and reaction path models on seafloor heat and mass transfer processes. *Geochimica et Cosmochimica Acta*, 163:59–79. <https://doi.org/10.1016/j.gca.2015.04.040>
- Stüeken, E.E., Anderson, R.E., Bowman, J.S., Brazelton, W.J., Colangelo-Lillis, J., Goldman, A.D., Som, S.M., and Baross, J.A., 2013. Did life originate from a global chemical reactor? *Geobiology*, 11(2):101–126. <https://doi.org/10.1111/gbi.12025>
- Suhr, G., Hellebrand, E., Johnson, K., and Brunelli, D., 2008. Stacked gabbro units and intervening mantle; a detailed look at a section of IODP Leg 305, Hole U1309D. *Geochemistry, Geophysics, Geosystems*, 9(10):Q10007. <https://doi.org/10.1029/2008GC002012>
- Summit, M., and Baross, J.A., 2001. A novel microbial habitat in the mid-ocean ridge seafloor. *Proceedings of the National Academy of Sciences of the United States of America*, 98(5):2158. <https://doi.org/10.1073/pnas.051516098>
- Sylvan, J.B., Estes, E.R., Bogus, K., Colwell, F.S., Orcutt, B.N., and Smith, D.C., 2021. Technical Note 4: Recommendations for microbiological sampling and contamination tracer use aboard the JOIDES Resolution following 20 years of IODP deep biosphere research. *International Ocean Discovery Program*. <https://doi.org/10.14379/iodp.tn.4.2021>

- Ternieten, L., Früh-Green, G.L., and Bernasconi, S.M., 2021. Distribution and sources of carbon in serpentinized mantle peridotites at the Atlantis Massif (IODP Expedition 357). *Journal of Geophysical Research: Solid Earth*, 126(10):e2021JB021973. <https://doi.org/10.1029/2021JB021973>
- Titarenko, S.S., and McCaig, A.M., 2016. Modelling the Lost City hydrothermal field: influence of topography and permeability structure. *Geofluids*, 16(2):314–328. <https://doi.org/10.1111/gfl.12151>
- Tucholke, B.E., Behn, M.D., Buck, W.R., and Lin, J., 2008. Role of melt supply in oceanic detachment faulting and formation of megamullions. *Geology*, 36(6):455–458. <https://doi.org/10.1130/G24639A.1>
- Tutolo, B.M., Luhmann, A.J., Tosca, N.J., and Seyfried, W.E., 2018. Serpentinization as a reactive transport process: the brucite silicification reaction. *Earth and Planetary Science Letters*, 484:385–395. <https://doi.org/10.1016/j.epsl.2017.12.029>
- Wang, D.T., Reeves, E.P., McDermott, J.M., Seewald, J.S., and Ono, S., 2018. Clumped isotopologue constraints on the origin of methane at seafloor hot springs. *Geochimica et Cosmochimica Acta*, 223:141–158. <https://doi.org/10.1016/j.gca.2017.11.030>
- Whattam, S.A., Früh-Green, G.L., Cannat, M., De Hoog, J.C.M., Schwarzenbach, E.M., Escartin, J., John, B.E., Leybourne, M.I., Williams, M.J., Rouméjon, S., Akizawa, N., Boschi, C., Harris, M., Wenzel, K., McCaig, A., Weis, D., and Bilenker, L., 2022. Geochemistry of serpentinized and multiphase altered Atlantis Massif peridotites (IODP Expedition 357): petrogenesis and discrimination of melt-rock vs. fluid-rock processes. *Chemical Geology*, 594:120681. <https://doi.org/10.1016/j.chemgeo.2021.120681>
- Wheat, C.G., Kitts, C., Webb, C., Stolzman, R., McGuire, A., Fournier, T., Pettigrew, T., and Jannasch, H., 2020. A new high-temperature borehole fluid sampler: the Multi-Temperature Fluid Sampler. *Scientific Drilling*, 28:43–48. <https://doi.org/10.5194/sd-28-43-2020>

Site summaries

Site AMDH-01A

Priority:	Primary
Legacy hole:	Sample and deepen Hole U1309D
Position:	30.1687°N, 42.1186°W
Water depth (m):	1656
Target drilling depth (mbsf):	2060
Approved maximum penetration (mbsf):	2100 (discretion of the shipboard party to deepen the hole if time is available)
Objective(s):	<ul style="list-style-type: none"> • Sample fluids and measure temperature in existing Hole U1309D to 1414 mbsf (expected temperature: 225°C) • Deepen existing Hole U1309D ~680 m and collect samples for petrology and geochemistry of abiotic organic compounds and H₂ • Log Hole U1309D with flasked tools • Drill new 80 m hole 20–30 m north of Hole U1309D, for microbiology sampling of porous rocks, fault zones, and correlation with Holes U1309B and U1309D (new hole was designated "U1309-J" in Proposal 937 text and site form)
Coring program:	RCB core Hole U1309D to 2100 mbsf Spud and RCB core a new hole ("U1309J")
Downhole measurements program:	<ul style="list-style-type: none"> • Sample fluids with new MTFs and Kuster FTS tools • Log temperature • Log newly drilled hole with flasked tools
Nature of rock anticipated:	Gabbroic and ultramafic rocks in Hole U1309D; diabase (dolerite) sills, altered gabbros, and fault rocks in new hole ("U1309J")

Site AMDH-02A

Priority:	Primary
Position:	30.1317°N, 42.1202°W
Water depth (m):	825
Target drilling depth (mbsf):	Pilot hole: 50–100 (single bit) Reentry hole: ~200 (2 bits)
Approved maximum penetration (mbsf):	800 (discretion of the shipboard party to deepen the hole if time is available)
Objective(s):	<ul style="list-style-type: none"> • 200 m hole with reentry system • Complete section through detachment fault zone in serpentinized peridotite • Sample for deformation, alteration, igneous petrology, microbiology, and organic/inorganic geochemistry • Log for temperature and other properties • Legacy hole for sampling fluids and gases, establishing temperature profile, potential instrumentation
Coring program:	Pilot hole: Hard rock spud in with RCB Main hole: Set HRT reentry system and then RCB
Downhole measurements program:	<ul style="list-style-type: none"> • Standard tool suites • Fluid sampling with Kuster FTS tool
Nature of rock anticipated:	Serpentinite and gabbroic and basaltic rocks

Site AMDH-03A

Priority:	Alternate
Legacy hole:	Reentry system for future operations
Position:	30.1389°N, 42.1455°W
Water depth (m):	1275
Target drilling depth (mbsf):	200
Approved maximum penetration (mbsf):	800 (discretion of the shipboard party to deepen the hole if time is available)
Objective(s):	<ul style="list-style-type: none"> • Drill through detachment fault shear zone • Sample for igneous petrology, alteration, deformation fabrics, microbiology, and organic geochemistry • Potential for postdetachment volcanic rocks • Temperature profile, fluid sampling, potential to provide reentry system for legacy
Coring program:	Pilot hole: Hard rock spud in with RCB Main hole: Set HRT reentry system and then RCB
Downhole measurements program:	<ul style="list-style-type: none"> • Standard tool suites • Fluid sampling with Kuster FTS tool
Nature of rock anticipated:	Gabbroic, basaltic, and fault rocks

Site AMDH-05A

Priority:	Alternate
Legacy hole:	None
Position:	<p>Polygon defined by 12 points:</p> <ul style="list-style-type: none"> • 30.13°N, 42.188°W • 30.13333°N, 42.17°W • 30.12367°N, 42.15833°W • 30.12667°N, 42.12°W • 30.129°N, 42.1125°W • 30.1225°N, 42.09417°W • 30.13°N, 42.09533°W • 30.13367°N, 42.115°W • 30.13583°N, 42.1225°W • 30.145°N, 42.12167°W • 30.15°N, 42.14167°W • 30.145°N, 42.18333°W
Water depth (m):	~1000 (but variable within approved area)
Target drilling depth (mbsf):	100
Approved maximum penetration (mbsf):	205 (discretion of the shipboard party to deepen the hole if time is available)
Objective(s):	<ul style="list-style-type: none"> • Series of single-bit holes • Near complete section through detachment fault zone in serpentinized peridotite • Sample for deformation, alteration, igneous petrology, microbiology, and organic/inorganic geochemistry • Log for temperature and other properties • Alternate site if operations fail at main sites
Coring program:	<p>Multiple hard rock spud in with RCB Single bit</p>
Downhole measurements program:	<ul style="list-style-type: none"> • Standard tool suites • Fluid sampling with Kuster FTS tool
Nature of rock anticipated:	Gabbroic, basaltic, and fault rocks